

1 **A Review of Fluid Inclusion Constraints on Mineralization in the Irish Orefield**  
2 **and Implications for the Genesis of Sediment-Hosted Zn-Pb deposits**

3  
4 J.J. Wilkinson

5  
6 CODES, University of Tasmania, Private Bag 126, Hobart, Tasmania 7001, Australia

7  
8 and

9  
10 Department of Earth Science and Engineering, Imperial College London, South Kensington Campus,  
11 Exhibition Road, London SW7 2AZ, UK

12  
13  
14 **Abstract**

15  
16 Many fluid inclusion studies have been carried out in the Irish Midlands Basin orefield (Lower  
17 Carboniferous) since the earliest work by Ed Roedder in the late 1960s. Results show that, in the ore  
18 deposits, the total range in fluid salinity is 4-28 wt% NaCl equivalent but with the majority falling in  
19 the moderate salinity range between 8-19 wt%. This variability is interpreted in terms of mixing  
20 between moderate salinity ore fluids and low temperature brines during ore formation. The most  
21 northerly ore deposits of Navan and Abbeytown are distinct in containing fluids of both lower and  
22 higher salinity than is typical of the Waulsortian-hosted deposits further south (Tynagh, Silvermines,  
23 Lisheen and Galmoy). Subeconomic prospects tend to display a narrower range in salinity, mostly at  
24 the lower end of the range observed in the ore deposits. In some prospects, and on the margins of  
25 some ore deposits, evidence for dilution is observed, interpreted to reflect mixing between  
26 hydrothermal fluids and unmodified seawater. This process is inferred to be unfavorable for  
27 mineralization.

28 Homogenization temperatures, a reasonable proxy for true trapping temperatures in the orefield,  
29 range from 70-280 °C but with the majority falling between 130-240 °C. There is no evidence for  
30 systematic stretching or leakage of inclusions related to the post-entrapment heating implied by  
31 elevated thermal maturity indicators. The highest temperatures are observed in the Waulsortian-  
32 hosted systems, with peak temperatures of ~280 °C supported by local, high grade Cu and Ni  
33 mineralization. In the Navan and Abbeytown deposits, lower temperature fluids appear to have been  
34 more prevalent. The subeconomic prospects formed over essentially the same temperature range as

35 the ore deposits (90-270 °C), with the exception of the morphologically and texturally distinct MVT  
36 systems in the region (e.g., Kinnitty, Harberton Bridge) that formed at lower temperatures (50-100  
37 °C).

38 Similar hydrothermal fluids to those recorded in both deposits and prospects are widely observed  
39 in dolomite (and sometimes calcite) cements within Courceyan-Arundian age rocks indicating  
40 hydrothermal fluid activity occurred over an extremely large area (>30,000 km<sup>2</sup>) and probably over  
41 an extended time period. There is a broad regional division in fluid properties suggesting that the  
42 northwestern and southeastern provinces, separated by the trace of the lapetus suture zone, may  
43 represent partly decoupled, large-scale flow regimes. Up to three, low temperature brine types are  
44 also recorded by cements in the host rock sequence, indicating a complex range of evaporation and  
45 fluid-rock interaction processes were ongoing in the shallow basin succession during the period of  
46 hydrothermal activity.

47 Halogen data show that fluids involved in mineralization were originally seawater-derived brines,  
48 produced by evaporation to varying degrees. Relatively high temperature, basement-interacted  
49 hydrothermal fluids were derived from partially evaporated seawater (molar Cl/Br = 559-825). Their  
50 compositions can be explained by dolomitization in the Carboniferous succession prior to circulation  
51 to depth; alkali exchange, reduction and metal-leaching from the Lower Paleozoic basement; and  
52 mixing with low temperature brines that locally penetrated the upper parts of the basement rock  
53 package. Fertile ore fluids appear to be characterized by higher  $\delta^{18}\text{O}$  (+7 to +9 ‰), lower  $\delta\text{D}$  (-25 to -  
54 45 ‰) and much higher metal contents than otherwise similar fluids sampled in basement-hosted  
55 feeder veins distal to deposits. This may reflect highly efficient metal scavenging in deeper/higher  
56 temperature reaction zones that underlie the principal deposits. In the ore deposits, these fluids  
57 mixed with Br-enriched bittern brines (Cl/Br ~290) produced by evaporation of Carboniferous  
58 seawater past halite saturation. It is inferred that bittern brine generation occurred in the shallow  
59 marine shelf regions in the footwalls to the synsedimentary fault systems that controlled the  
60 localization of mineralization. These brines then migrated into hangingwall depressions where they  
61 ponded within permeable sediments and became enriched in H<sub>2</sub>S via bacteriogenic sulfate reduction.  
62 The coincidence of structurally-controlled, high temperature reaction zones, brine-producing  
63 footwalls, and hangingwall traps, with bacterial blooms above upwelling plumes of hydrothermal  
64 fluids, can be interpreted as a self-organizing system that locally converged on ore-forming  
65 conditions. Understanding the first-order structural control of the ore systems will therefore be  
66 critical for predicting new deposits.

67 The Irish orefield presents arguably the best database available on the thermal and chemical  
68 characteristics of hydrothermal fluids involved in sediment-hosted ore genesis. The system shares  
69 much of the variety and complexity observed in other intracratonic basin-hosted Zn-Pb(-Ba) ore

70 districts. This includes the coexistence of contrasting styles of mineralization that are typically  
71 observed in the more distal and platform-marginal parts of the basinal environment. The thermal  
72 and chemical fluid heterogeneity observed is typical of modern intracratonic basin systems and  
73 should be expected in large paleohydrothermal systems where recharge of surface-derived fluids is  
74 involved.

75

76

## Introduction

77

78 The Carboniferous Irish Midlands Basin hosts a remarkable concentration of base metals (~17 MT  
79 known) in a prospective area of approximately 200x150 km. In addition to the known prospects,  
80 operating mines at Navan, Lisheen and Galmoy, and the historical mines at Tynagh, Silvermines and  
81 Abbeystown, anomalous concentrations of Zn and Pb are common in the lower part of the  
82 Waulsortian Limestone Formation and pervasive in the Navan Group – the primary host rock  
83 sequences (Blakeman, pers. comm.). Such extensive mineralization implies the operation of a giant  
84 hydrothermal system of significant academic as well as economic interest. Indeed, the orefield has  
85 been important in a number of debates on the classification of sediment-hosted deposits and the  
86 nature of the hydrothermal systems that form them (Russell, 1978; Russell et al., 1981; Hitzman and  
87 Large, 1986; Lydon, 1986; Hitzman and Beaty, 1996; Everett et al., 2003; Wilkinson, 2003; Leach et  
88 al., 2005; Wilkinson et al., 2005a).

89 The purpose of this paper is to provide a historical review of fluid inclusion studies carried out in  
90 the Irish orefield, including investigations of individual mineralized systems (deposits and prospects)  
91 as well as regional studies in the host rock stratigraphy and underlying basement. The contribution of  
92 these data to the development of genetic models for mineralization is highlighted. Previously  
93 unpublished data are also presented that, in combination with the published results, provide an  
94 extensive dataset that constrains the nature of the fluid regimes operating in the region prior to,  
95 during, and subsequent to the main stages of ore formation. How these data impact on our  
96 understanding of the Irish paleohydrothermal system and the wider implications for models of  
97 sediment-hosted ore formation are considered.

98

99

## Geological Setting and Mineralization

100

101 A thorough description of the geology and mineralization in Ireland is beyond the scope of this  
102 contribution and only a brief summary is presented here. For more detail and thorough reviews the  
103 reader is referred to Andrew et al. (1986), Hitzman and Large (1986), Phillips and Sevastopulo (1986),

104 Bowden et al. (1992), Andrew (1993), Anderson et al. (1995), Hitzman (1995), Hitzman and Beaty  
105 (1996), and Kelly et al. (2003).

106 Zinc-lead mineralization in the Irish Midlands is hosted by Lower Carboniferous (Dinantian)  
107 carbonate rocks (Fig. 1), within both the Waulsortian Limestone Formation and the Navan Group –  
108 the first major non-argillaceous carbonate units in a transgressive marine sequence. Beneath these  
109 rocks lie red, terrestrial mudstones, sandstones and conglomerates (Old Red Sandstone, ORS) that in  
110 turn unconformably overlie an eroded Lower Paleozoic volcanosedimentary succession that was  
111 deformed and underwent low grade metamorphism in the Caledonian Orogeny. A crystalline  
112 basement is inferred at depth in the Midlands area (Strogen, 1974; Kennan et al., 1979) and likely  
113 comprises Grenvillian gneiss and schist to the northwest and late Precambrian, probably Avalonian,  
114 gneissic rocks to the southeast (Watson, 1978; Phillips and Sevastopulo, 1986).

115 The Waulsortian Limestone Formation developed in a ramp environment in the Courceyan as  
116 biomicrite mounds surrounded by argillaceous bioclastic limestones (ABL) at moderate water depths  
117 of up to several hundred meters. Waulsortian banks dominate in the south and west Midlands,  
118 where they coalesced to form thicknesses in excess of 750 m (Andrew, 1993) in the Shannon Trough  
119 (Fig. 1). The Navan Group, of similar age, comprises near-shore, shallow marine, largely high-energy  
120 deposits, including oolitic and bioclastic grainstones, birdseye micrites and minor sandstones  
121 (Philcox, 1984). These were deposited in the northern Midlands on the southern margin of the  
122 Laurasian landmass, now marked by the Longford Down inlier (Fig. 1).

123 The host rocks underwent early diagenesis that included extensive calcite cementation and  
124 dolomitization (Lees and Miller, 1995; Rizzi and Braithwaite, 1997; Gregg et al., 2001; Lee and  
125 Wilkinson, 2002; Wilkinson, 2003; Nagy et al., 2004). It is widely considered that these processes  
126 were initiated upon deposition of the carbonate sediments, with significant cementation occurring  
127 within a few tens of meters of the seafloor (cf. Dix and Edwards, 1996). Early dolomitization is  
128 pervasive in the southeastern Midlands, fringing the Leinster Massif (Phillips and Sevastopulo, 1986;  
129 Hitzman and Beaty, 1996; Gregg et al., 2001; Nagy et al., 2004), but is also widely developed  
130 elsewhere (Gregg et al., 2001). Sulfides appear to generally postdate early dolomite cements and are  
131 themselves accompanied by a variety of replacive, breccia-cementing and vein- and vug-filling calcite  
132 and dolomite, plus variable barite and minor quartz (Fig. 2).

133 Mineralization in the ore deposits principally occurs as massive sulfide displaying a complex range  
134 of textures (Boast et al., 1981; Taylor, 1984; Ashton et al., 1986; Anderson et al., 1998; Hitzman et al.,  
135 2002; Fuscuardi et al., 2003; Lowther et al., 2003; Wilkinson et al., 2005b). In sub-economic  
136 mineralization, a variety of massive, disseminated, breccia- and vein-filling styles occur (e.g.  
137 Holdstock, 1982; Emo, 1986; Grennan, 1986; Trude and Wilkinson, 2001). Abundant ore minerals are  
138 sphalerite, galena and pyrite, with lesser but variable marcasite and minor chalcopyrite, tennantite

139 and other sulfosalts. Orebodies are broadly stratiform but in most cases have been shown to be  
140 strictly stratabound and occur as single or multiple lenses hosted by favorable horizons within the  
141 hostrock packages. For the deposits of Lisheen and Galmoy, this is a breccia unit of variable  
142 thickness, located close to the base of the Waulsortian Limestone.

143

#### 144 **The Reliability of Fluid Inclusion Data**

145

146 A fundamental assumption in fluid inclusion studies is that inclusions have maintained their integrity  
147 since their time of formation (Roedder, 1984). In the Irish Midlands, the validity of fluid inclusion  
148 data has been questioned by some authors (Hitzman, 1995; Hitzman and Beaty, 1996; Peace, 1999;  
149 Reed and Wallace, 2001) because vitrinite reflectance and conodont color analyses suggest that the  
150 Carboniferous rocks have been subject to late Carboniferous heating (Clayton et al., 1989). The  
151 highest maturation values are observed in the Munster Basin in southern Ireland where Variscan  
152 deformation and metamorphism have occurred. However, high values extend into the southeast and  
153 west Midlands where, taken at face value, vitrinite reflectance values ( $R_m > 4\%$ ) imply peak  
154 temperatures in excess of 300 °C and conodont alteration indices (CAI) of 5-7 imply temperatures of  
155 300 to >550 °C. Any re-equilibration toward lower density (greater inclusion volume) by plastic  
156 stretching, or partial leakage of inclusions, as a result of overheating would result in anomalously  
157 high homogenization temperature ( $T_h$ ) values and an overestimate of ore fluid temperatures. Thus,  
158 although no textural evidence for inclusion re-equilibration (e.g. Bodnar, 2003a) has been described  
159 from the Irish Midlands, it is nonetheless important to consider this issue before discussing the data  
160 in detail.

161 Laboratory studies have shown that the potential for inclusion re-equilibration during overheating  
162 is largely a function of inclusion size and host mineral strength (e.g. Bodnar and Bethke, 1984;  
163 Burruss, 1987; Bodnar et al., 1989). Consequently, a plot of inclusion size against  $T_h$  should show a  
164 positive correlation if partial re-equilibration has occurred and this effect would be more pronounced  
165 for softer minerals in which inclusions can deform under lower internal overpressures (e.g. calcite,  
166 barite). In addition, modification is more likely to affect some inclusions in a given inclusion  
167 assemblage than others due to variations in size, shape, or proximity to defects. This would result in  
168 variable  $T_h$  data within individual inclusion populations and the elimination of systematic differences  
169 between different growth stages of a single mineral grain, or between different paragenetic stages.

170 The first application of a size/ $T_h$  test for different host minerals was presented by Everett et al.  
171 (1999a) for data from Lower Paleozoic-hosted veins. These data are supplemented here and  
172 compared with results from regional carbonates and deposits (Fig. 3A). For all datasets (with the  
173 possible exception of deposit barite), no positive correlation is apparent for any mineral host.

174 Sphalerite and quartz are the strongest host minerals and therefore might be expected to preserve a  
175 putative lower temperature population, especially in smaller inclusions. In fact, the opposite is  
176 observed, with these minerals generally hosting higher  $T_h$  inclusions. The broad  $T_h$  differences  
177 between the minerals (quartz>calcite>dolomite>pink dolomite) and the notable bimodality in  
178 sphalerite values cannot be easily explained by re-equilibration and are likely to reflect features of  
179 genetic significance, principally differences in precipitation temperature.

180 A similar plot for regional Lower Carboniferous carbonates (Fig. 3B) again shows no size- $T_h$   
181 correlation, appears to show a bimodality in dolomite data, and illustrates low  $T_h$  values in the  
182 weakest mineral, calcite.

183 For the deposit data, sphalerite  $T_h$  values are the highest, followed by dolomite and then calcite –  
184 the opposite of what might be expected for stretching populations. At some of the prospects (e.g.  
185 Harberton Bridge; Trude and Wilkinson, 2001) calcite hosts monophase inclusions that could not  
186 have been preserved if post-entrapment temperatures had exceeded 300 °C. Barite also contains  
187 monophase inclusions at some localities (e.g. Silvermines; Samson and Russell, 1987) that would be  
188 impossible to preserve during such overheating. However, variable degrees of filling are commonly  
189 observed in barite and a weak positive correlation between size and  $T_h$  is observed in the deposit  
190 data (Fig. 3C) suggesting leakage (during post-entrapment burial or laboratory analysis) is a problem  
191 for this mineral. Consequently,  $T_h$  data (but not necessarily compositional information) from barite  
192 are treated as generally unreliable (cf. Bodnar and Bethke, 1984; Ulrich and Bodnar, 1988).

193 The last, and perhaps most convincing, evidence for preservation of inclusion integrity is the  
194 petrography which demonstrates that individual inclusion populations (such as within a single  
195 dolomite growth zone) typically display a relatively narrow range of  $T_h$  values that is much less than  
196 within a sample as a whole, or between samples. Furthermore, systematic variations in  
197 microthermometric data can be observed that relate to changes in fluid properties during crystal  
198 growth (Fig. 4). These features would not be preserved if post-entrapment re-equilibration was  
199 widespread.

200 The contradiction between Devonian and Carboniferous maturation data and Lower  
201 Carboniferous fluid inclusion data is problematic. Although higher temperatures are plausible in the  
202 Munster Basin to the south, where the rocks have been subjected to Variscan thrusting and have  
203 developed a cleavage, it is difficult to credit rock temperatures of up to 550 °C in the Midlands Basin,  
204 (except immediately adjacent to minor intrusions) given the lack of evidence for recrystallization at  
205 such high temperatures, lack of mineralogical indicators, and perfect preservation of delicate fossils  
206 and low-temperature diagenetic fabrics. Consequently, it has been suggested that CAI and  $R_m$  values  
207 recorded in the Midlands do not reflect true maximum temperatures (Everett, 1999; Wilkinson et al.,  
208 2003). The reason for this is uncertain, although it is most likely due to hydrothermal overprinting

209 (e.g. Rejebian et al. 1987) by the unusually extensive flow that has affected much of the stratigraphy  
210 in the Midlands area, and which may have been active over a long period of time (e.g. Hitzman, 1995;  
211 Wright et al. 2000; Gregg et al. 2001; Wilkinson, 2003).

212 The modification of CAI values by fluids is suggested by a number of features of the dataset  
213 presented by Clayton et al. (1989). In particular, reddened limestones, commonly inferred to be  
214 related to hydrothermal activity (Hitzman et al., 1995), display elevated CAI values of 6-7 compared  
215 with values of 5-5.5 in normal limestones from the same drillhole or nearby (e.g. Meelin No.1  
216 borehole, Co. Cork; Rocky Island, Co. Cork; Fig. 1). Also, dolomitized intervals can display higher CAI  
217 than undolomitized intervals in the same drillhole (e.g. Ballyragget No. 1 borehole, Co. Kilkenny) and  
218 there is often a variation of up to 1 CAI in single samples. Local vertical reversals in thermal gradients  
219 down boreholes also suggest a complex thermal regime probably involving advective heating  
220 (Goodhue and Clayton, 1999). This conclusion is supported by Jones (1992) who noted that CAI  
221 values in Ireland are influenced by proximity to major mineral deposits and follow Caledonoid trends,  
222 these structures also being implicated as the major infrabasinal flow conduits. Numerical modeling  
223 has shown that anomalous organic maturity can be accounted for by free thermal convection in the  
224 continental crust beneath intracratonic basins (Nunn, 1994). Consequently, the weight of evidence  
225 supports widespread preservation of fluid inclusion integrity in the Midlands area and therefore in  
226 the discussion below  $T_h$  values are considered reliable except where standard petrographic evidence  
227 indicates otherwise.

228

229

230

### **Historical Review of Fluid Inclusion Studies**

231

232 Fluid inclusion studies in the Irish orefield have played an important part in the development of  
233 genetic models and the debate surrounding the timing and depth of mineralization. Opposing views  
234 can be distilled down to purely epigenetic models invoking largely lateral fluid flow and replacement/  
235 cavity-filling mineralization at depth, during burial, from fluids close to thermal equilibrium with their  
236 host rocks (Hitzman and Beaty, 1996; Reed and Wallace, 2001; Peace et al., 2003); and SEDEX  
237 models, in which near-seafloor and underlying epigenetic mineralization occurred during diagenesis  
238 of the host rocks from elevated temperature fluids in the updrafts of a convective flow system  
239 (Boyce et al., 1983; Russell, 1978, 1986). The more recent evidence that much mineralization  
240 probably formed by host rock replacement in the shallow sub-seafloor environment (Anderson et al.,  
241 1998; Blakeman et al., 2002; Lee and Wilkinson, 2002; Wilkinson et al., 2003, 2005a, 2005b) and a  
242 relaxed definition of the term "SEDEX" (Leach et al., 2005) means that the deposits can be classified  
243 as carbonate-replacement SEDEX type.

244 In the following review, only fluid inclusions interpreted to be of primary (or pseudosecondary)  
245 origin and constrained paragenetically to be associated with the principal mineralizing stages are  
246 considered, except where otherwise stated. In the summary of fluid properties (Table 1), the modes  
247 and ranges given are considered to be the best reliable estimates based on published information;  
248 these may omit outlying data which are noted and, in some cases, have necessitated a degree of  
249 interpretation of results that may be equivocal. Most of the results discussed are salinity data  
250 inferred from final ice melting (as the last solid phase), or in some cases hydrate melting  
251 temperatures ( $T_{mhyd}$ ), together with  $T_h$  values which, in the Irish system, can be considered to be a  
252 reasonable proxy for trapping temperatures (e.g. Wilkinson and Earls, 2000). Additional chemical or  
253 isotopic data acquired from fluid inclusion analyses are also discussed.

254

### 255 *Ore Deposits*

256 It is appropriate for this volume that the history of fluid inclusion research in Ireland was started  
257 by Ed Roedder himself in the late 1960s. The earliest data reported, obtained on sphalerite from the  
258 Keel deposit (Fig. 1), are attributed variously in the literature but were in fact acquired by Ed Roedder  
259 (unpublished USGS memorandum to T.B. Nolan, 1968), listed in Roedder (1976), on samples  
260 collected by Nolan on a visit to the deposit. Patterson (1970) cites these data and quotes from  
261 Roedder's report:

262

263 *"The samples had clear euhedral, yellow to brown, unzoned sphalerite crystals up to 8 mm as a crust*  
264 *on [Lower Paleozoic] quartzite. These sphalerite crystals contained reasonably good primary and*  
265 *pseudo secondary fluid inclusions yielding the following data: (no distinction in the measurements*  
266 *could be made between the two types of inclusions):*

267

268 *Freezing temperatures: 10 inclusions all between  $-7.35 \pm 0.5$  and  $-8.0 \pm 0.2$  °C*

269 *1 inclusion  $-6.0 \pm 0.1$  °C*

270 *Filling [homogenization] temperature: 3 inclusions  $176 \pm 5$  °C*

271 *5 inclusions  $185 \pm 3$  °C*

272

273 *Thus this sample (if not the whole deposit), formed from rather hot brines, with a salinity in the range*  
274 *of 11-12 per cent salts in solution."*

275

276 These were the first data to shed light on the nature of the fluids responsible for formation of the  
277 Irish deposits and suggested that they formed at higher temperatures and from lower salinity fluids  
278 than those typical of carbonate-hosted deposits of Mississippi Valley-type (MVT).



279 Early results were also reported by Greig et al. (1971) from Silvermines. Only three datapoints  
280 (possibly averages of individual samples) were presented on a plot of  $T_h$  vs. distance from the  
281 Silvermines fault zone; these indicated  $T_h$  values of 190-280 °C for inclusions hosted by quartz,  
282 sphalerite and barite. Further reconnaissance results were presented by Probert (1983; cited in  
283 Andrew, 1993) from locations in the northern Midlands including the Navan deposit and the Keel,  
284 Moyvoughly and Tatestown prospects (Fig. 1). The absence of paragenetic or spatial control makes  
285 interpretation of these results risky, but some comparisons with subsequent studies can be made  
286 (Table 1). More recent and carefully-constrained results from Navan (this study) do not replicate  
287 these early measurements although it should be noted that the high grade core of the deposit was  
288 mined out in the 1980s-1990s.

289 *Silvermines*: The first detailed fluid inclusion study was carried out principally on the lower  
290 (epigenetic) orebodies and Old Red Sandstone-hosted footwall veins from the Silvermines deposit  
291 (Samson, 1983; Samson and Russell, 1983). Homogenization temperature and salinity data (modelled  
292 in the NaCl-H<sub>2</sub>O system) were reported from inferred primary and pseudosecondary liquid-vapor  
293 fluid inclusions in quartz, sphalerite, calcite and dolomite, and salinity data from the predominantly  
294 monophasic liquid inclusions in barite. Extended results, including the addition of the first bulk  
295 analytical (crush-leach) chemical and isotopic (decrepitation, crushing) data and the observation and  
296 identification of trapped phases (calcite) in some inclusions were presented in a comprehensive,  
297 benchmark study by Samson and Russell (1987).

298 Wide ranges in microthermometric properties were observed (Table 1) and the occurrence of  
299 some vapor-rich inclusions in quartz was taken as evidence for episodic boiling; similar inclusions in  
300 carbonate and barite were discounted. Since then, vapor-rich inclusions have not been reported  
301 from the orefield (apart from in one Lower Paleozoic basement-hosted vein sample; Everett et al.,  
302 1999a) so it is likely that boiling was not a common process in the district (Wilkinson et al., 2003). A  
303 broad negative correlation between  $T_h$  and salinity was interpreted as the first direct evidence for  
304 fluid mixing in the Irish deposits, previously suggested based on sulfur isotope data and the chemical  
305 conditions of sulfide deposition (Boast et al., 1981). An important detail within this correlation is that  
306 samples from different geographic locations and paleodepths within the system tend to fall in  
307 different parts of the array, consistent with a relatively stable mixing zone between higher  
308 temperature, less saline fluids at depth (and possibly also on the fringes of the system) and more  
309 saline, cooler fluids higher up and in the center, proximal to the main ore zones.

310 *Tynagh*: Tynagh, the first Zn-Pb deposit to be discovered in the Lower Carboniferous of the  
311 Midlands Basin, was the subject of a fluid inclusion study by Banks and Russell (1992). Primary and  
312 secondary inclusion data were reported from limestone-hosted vein sphalerite from epigenetic  
313 mineralization in Zones 2 and 3, the principal ore zones in the deposit (Boast et al., 1981), together

314 with results from barite (monophase liquid inclusions predominant) and quartz (Table 1). Quartz-  
315 hosted inclusions were measured both from rare, euhedral quartz replacing carbonates in the ore  
316 zones and in quartz overgrowths in the ORS within 1 m of the Tynagh Fault in the deposit footwall.  
317 Although there is some ambiguity in the timing of these overgrowths, the inclusions were interpreted  
318 as relating to the main stages of ore formation.

319 As with Silvermines, a negative correlation was observed between  $T_h$  and salinity in the inferred  
320 ore-stage fluids, interpreted in terms of fluid mixing. The principal spread in salinities occurs in the  
321 footwall quartz overgrowths and in barite implying that these either formed during mixing, and/or  
322 were overprinted by fluids undergoing mixing. By contrast, and similar to Silvermines, the sphalerite  
323 data show little spread in salinity suggesting precipitation under somewhat different conditions. Data  
324 from quartz within the ores were not fully reported.

325 Banks and Russell (1992) also presented data from “post-ore” calcites that hosted four inclusion  
326 types. Because the paragenesis of the samples and the petrography of the inclusions within them are  
327 not described it is difficult to interpret these results. However, their Group 1 fluid inclusions ( $T_h$  109-  
328 196 °C; salinity 5.1-10.2 wt% NaCl equivalent;  $T_{m,hyd}$  -24.9 to -22.4 °C) coincide with the data  
329 reported by Probert (1983), as well as ore-stage fluids elsewhere (Table 1), and are therefore  
330 considered likely to be related to mineralization, although this was discounted by the authors. Some  
331 of the calcite samples were associated with a dolomite-chalcopyrite assemblage typical of the post-  
332 ore pink dolomite and later calcite widely developed in the Midlands Basin (the D<sub>5</sub> and C<sub>6</sub> of  
333 Wilkinson et al., 2005b; Fig. 2). This “copper dolomite” event is interpreted to represent a basin-wide  
334 brine migration, probably related to the onset, or relaxation, of Variscan compression (Andrew,  
335 1993; Wilkinson, 2003; Wilkinson et al., 2005b). The Group 3 inclusions of Banks and Russell (1992)  
336 are potentially associated with this stage based on similarities with microthermometric data from  
337 pink dolomite elsewhere (e.g. Eyre, 1998; Wilkinson, 2003). The Group 4 inclusions contained low  
338 salinity fluids and displayed anomalous hydrate melting behavior, with hydrate and ice coexisting  
339 above -20.8 °C, interpreted in terms of sulfate or bicarbonate presence. These are comparable to the  
340 dilute fluids typical of the C<sub>6</sub> cement stage (Fig. 2) that are strongly oxidizing and may therefore  
341 reflect groundwaters enriched in sulfate, possibly locally as a result of sulfide oxidation.

342 *Abbeytown*: The historic small mine of Abbeytown in Co. Sligo, studied by Hitzman (1986), lies  
343 well to the northwest of the main orefield (Fig. 1) and its genetic relationship to it remains enigmatic.  
344 A small number of two-phase fluid inclusions were analysed by R.J. Bodnar (cited in Hitzman, 1986)  
345 from the main mineralizing stage (sphalerite and calcite) and from late ore-stage calcite-pyrite  
346 breccias. These predominantly showed moderate salinities of 10-13 wt% NaCl equivalent, salinities  
347 that are typical of ore-related inclusions throughout the Midlands Basin.  $T_h$  values varied from 85-180  
348 °C with the majority in calcite falling at the upper end of this range and those in sphalerite at the

349 lower end. A minor population of more saline inclusions was also observed in ore-stage calcite but  
350 their timing was not discussed. No evidence for fluid mixing was observed and it was suggested that  
351 mineralization probably formed from a single fluid, perhaps due to cooling and/or neutralization by  
352 hostrock dissolution.

353 *Lisheen*: The discovery of Galmoy in 1986 (Doyle et al., 1992) focused exploration attention on the  
354 Rathdowney Trend in the southeast Midlands (Fig. 1), and proved a significant factor in the  
355 subsequent discovery of the Lisheen deposit (Hitzman et al., 1992). Initial fluid inclusion studies were  
356 reported in conference abstracts (Thompson et al., 1992; Eyre et al., 1996), with the first detailed  
357 results presented by Eyre (1998). In this study, fluid inclusion analyses from Galmoy, Lisheen and a  
358 number of prospects in the Rathdowney Trend were constrained with respect to the mineral  
359 paragenesis observed in the samples (see Wilkinson et al., 2005b for details), synthesized in Figure 2.

360 All analyzed fluid inclusions from Lisheen were of liquid-vapor type and showed simple low  
361 temperature phase behavior with first melting temperatures in the range -54 to -39 °C, best  
362 interpreted in terms of the NaCl-CaCl<sub>2</sub>-H<sub>2</sub>O system. Fluid inclusions in sphalerite showing permissive  
363 evidence for a primary origin displayed  $T_{m,hyd}$  of  $-22.6 \pm 0.3$  °C indicating the dominance of NaCl (e.g.,  
364 see Bodnar, 2003b). These yielded salinities mostly in the range 10.2-18.0 wt% NaCl equivalent. A  
365 marked polymodal distribution of salinities was observed (Table 1), including an unusually low  
366 salinity grouping from the outlying North Zone (Wilkinson et al., 2005b). Liquid-vapor  
367 homogenization temperatures (to the liquid) were mainly in the range 140-210 °C (up to 241 °C) with  
368 the highest mode observed for samples from the central Derryville Zone. Excluding the low salinity  
369 population, the groups define points along a trend of decreasing temperature and increasing salinity,  
370 similar to the data from Silvermines and Tynagh. Secondary, low  $T_h$  brine inclusions were commonly  
371 recorded.

372 Results from ore-stage and late ore-stage gangue phases fill out this trend with a more continuous  
373 data distribution. Measurements from a ferroan calcite-cemented "white matrix breccia" (drillhole  
374 LK262-100 m) from the Derryville Zone overlap most closely those from sphalerite. Rare data from  
375 quartz fall at the more saline end of the distribution. Data from post ore-stage pink dolomite (D<sub>5</sub>) and  
376 secondary inclusions in calcite veins (and in sphalerite) fall at the end of this array indicating the late-  
377 stage infiltration of low temperature brines into the deposit. Although these brines appear to  
378 represent a viable end-member for the suggested mixing process (Eyre, 1998; Wilkinson et al.,  
379 2005b), the pink dolomite itself is thought to significantly postdate mineralization and is related to  
380 extensive sulfide dissolution. Thus it is inferred that multiple brine types infiltrated the deposit  
381 during and subsequent to mineralization.

382 *Galmoy*: Fewer results are available from Galmoy but these show broadly similar characteristics to  
383 Lisheen (Table 1). Sphalerite data display several salinity clusters in the range 10.8-16.3 wt% NaCl

384 equivalent and a relatively narrow range of homogenization temperatures between 129-179 °C  
385 (Table 1), notably lower than at Lisheen. Hydrate melting was recorded in one sample at  $-22.4 \pm 0.2$  °C  
386 indicating predominance of NaCl over  $\text{CaCl}_2$ . Low  $T_h$  secondary inclusions were again common but no  
387 salinity data are available. The sphalerite data overlap significantly with results from white matrix  
388 breccia dolomite ( $D_3$ ; see Fig. 2), consistent with a syn- ore-stage timing for these breccias as inferred  
389 at Lisheen (Wilkinson et al., 2005b). Limited measurements on late ore-stage dolomite and calcite  
390 yielded a wide range in  $T_h$  (111-228 °C) and salinity but are consistent with the possible mixing trend  
391 defined at Lisheen.

392

### 393 *Subeconomic Prospects*

394 Studies of the subeconomic prospects in the orefield have been important in order to constrain  
395 relative timing of mineralization in less intensely altered environments and to compare geological  
396 characteristics with the larger systems to evaluate controls of economic mineralization. However, no  
397 systematic comparison of the characteristics of the fluids involved has been carried out.

398 *Keel:* The Keel prospect and the adjacent Garrycam barite deposit (Fig. 1) have been widely  
399 studied but never in great detail. The Keel deposit comprises stratabound breccia and fracture-fill  
400 mineralization, localized by faults, that is hosted in rocks extending from the uppermost Silurian  
401 basement slates up to the top of the Navan Group “Mixed Beds” (Slowey, 1986). It is distinctive in  
402 that much of the sulfides occur as relatively coarse, euhedral crystals cementing breccias.

403 Subsequent to the initial study by Roedder, both Probert (1983) and Thompson (1992; cited in  
404 Slowey et al., 1995) obtained  $T_h$  values in the range 110-187 °C and salinities of 11-24 wt% NaCl  
405 equivalent but without detailed paragenetic control. Higher  $T_h$  values from barite at Garrycam were  
406 considered to be unreliable. Later work reported data within this same range (Caulfield et al., 1986),  
407 confirmed in this study on primary inclusions hosted by color-zoned sphalerite (Table 1). Late, pale-  
408 yellow and transparent sphalerite trapped the coolest and lowest salinity fluids, interpreted to reflect  
409 dilution of earlier, more saline and Fe-rich fluids. This pattern is similar to that recognized in  
410 carbonate-base metal-gold epithermal deposits (Corbett, 2004). Post-sphalerite quartz contains the  
411 most dilute inclusions (4.4-9.1 wt% NaCl equivalent; Collins, unpublished MSci dissertation, Imperial  
412 College London, 2005; This study) suggesting that dilution eventually quenched ore formation. The  
413 polymodal salinities observed at Keel-Garrycam, lack of evidence for mixing (with the exception of  
414 the late dilution noted above), and range in  $T_h$  values suggest a complex history involving injection  
415 and cooling of a number of fluid pulses.

416 *Harberton Bridge:* Harberton Bridge, located in Co. Kildare in the eastern part of the Midlands  
417 (Fig. 1), is one of a number of small sulfide- and carbonate-cemented breccia deposits of Mississippi  
418 Valley-type (Holdstock, 1982). The Kildare District has been widely cited as hosting an end-member

419 of the spectrum of styles of deposit in the orefield (Andrew, 1993; Wilkinson, 2003). Marcasite and  
420 sphalerite are the dominant (commonly interbanded) sulfides with minor amounts of galena that  
421 sometimes shows a recrystallized dendritic form (Trude and Wilkinson, 2001). The typical  
422 paragenesis is early marcasite-calcite, often replacing or overgrowing limestone host rock, followed  
423 by polymetallic marcasite-sphalerite-galena-calcite mineralization overprinted by late calcite  
424 (Holdstock, 1982, 1983). Dolomite and pyrite are uncommon. This sequence is similar to that  
425 described for the other Kildare deposits by Dixon (1990).

426 Preliminary  $T_h$  measurements of  $\sim 100$  °C from Harberton Bridge were reported in a personal  
427 communication by Finlow-Bates, cited in Emo (1986). The only systematic study, on representative  
428 samples from one drillhole, found that monophasic primary and secondary inclusions were abundant  
429 in calcite, although two-phase inclusions of probable primary origin were also present (Trude and  
430 Wilkinson, 2001). These yielded  $T_h$  values of 48-70 °C with an average of 61.5 °C, interpreted to  
431 represent the upper end of the range likely for the calcite studied and indicating a very low  
432 temperature origin for this style of mineralization. Hydrate melting was sometimes observed, ranging  
433 from -37.2 to -21.8 °C, suggesting variable Ca:Na ratios. Salinities varied from 10.1 to 19.3 wt% NaCl  
434 equivalent, possibly indicative of mixing.

435 *Kinnitty*: The Kinnitty prospect, located on the northwestern flank of the Slieve Bloom inlier (Fig.  
436 1), is hosted by undolomitized Waulsortian Limestone and comprises stratabound calcite veins,  
437 calcite-cemented breccias, and cavity infillings. Iron sulfides are dominant, mainly layered marcasite-  
438 pyrite and melnikovite, and are typically interbanded with colloform sphalerite that contains galena,  
439 sometimes with dendritic habit. A later overprint of calcite-pyrite veins and breccia is also observed.

440 Calcite associated with sphalerite-galena-marcasite assemblages hosts two-phase inclusions with  
441  $T_h$  values of 45-80 °C and modal salinity of 20-21 wt% with a total range of 8-22 wt% NaCl equivalent  
442 (Table 1). Hydrate was commonly observed with a modal melting temperature of -21.3 °C indicating  
443 dominance of Na over Ca (Strongman, unpublished MSci Dissertation, Imperial College London,  
444 2001). The partial preservation of melnikovite, which converts to pyrite above 75 °C (Lepp, 1957), is  
445 consistent with the very low temperatures. The spread in salinity suggests mineralization could have  
446 been driven by mixing between a moderate salinity fluid ( $\sim 14$  wt%) and a more predominant brine  
447 ( $\sim 21$  wt%). Variable mixing proportions could account for the strongly oscillating chemistry and pH  
448 implied by the multiple interbanding of calcite(-melnikovite/pyrite) and marcasite.

449 *Cooleen*: The Cooleen Zone is a satellite of the Silvermines system (Lee and Wilkinson, 2002) that  
450 was explored by Ennex International in the 1990's before being abandoned as uneconomic.  
451 Mineralization is replacive and is focused within partially and wholly dolomitized sedimentary  
452 breccias. It comprises stratiform massive, semi-massive and disseminated sulfides dominated by  
453 pyrite with lesser sphalerite and minor galena. Galena is intimately associated with sphalerite,

454 sometimes forming bands of cubic crystals or dendrites located within and often at the core of  
455 growths of colloform sphalerite. Mineralized calcite and dolomite veins underlie and crosscut  
456 massive sulfides.

457 Fluid inclusion data were obtained from late ore-stage dolomite and calcite veins that cut massive  
458 sulfide mineralization and which have walls intermittently lined by euhedral, pale brown to orange-  
459 brown sphalerite and galena (Lee, 2002). Inclusions were usually two-phase liquid-vapor type,  
460 although monophasic inclusions were also observed in the calcite veins. A clear distinction was noted  
461 between inclusions hosted by dolomite (modal  $T_h = 180-190$  °C; salinity = 10.8-17.6 wt% NaCl  
462 equivalent) and calcite (modal  $T_h = 150-160$  °C; 4.8-14.2 wt% NaCl equivalent) with the former data  
463 showing a cluster and the latter displaying a trend from this cluster toward lower  $T_h$  and salinity  
464 values, interpreted to represent dilution. The few sphalerite-hosted inclusions measured fell into two  
465 groups: vein-hosted sphalerite contained inclusions comparable to those hosted by dolomite  
466 whereas a fragment of sphalerite interpreted to be a reworked clast in a sedimentary breccia hosted  
467 inclusions with much lower  $T_h$  and salinity values (Table 1).

468 *Rathdowney Trend:* In the Rathdowney Trend (Fig. 1), prospects at Holycross, Durrow and  
469 Rathdowney East were sampled for reconnaissance studies by Eyre (1998). A variety of  
470 mineralization styles are observed, principally disseminated, replacement and fracture-fillings  
471 associated with hydrothermal black ( $D_2$ ) and white ( $D_3$ ) dolomite.

472 Sphalerite- and vein dolomite-hosted inclusions from Holycross display a prominent mode in  $T_h$  at  
473 170-180 °C with salinity modes at 10-11 and 16-17 wt% NaCl equivalent (Table 1), very similar to  
474 Lisheen. Hydrate melting was observed at -22.7 °C, identical to Lisheen and Galmoy sphalerites  
475 (Table 1). Relatively high and variable homogenization temperatures of 155-267 °C (principal mode  
476 210-220 °C) were recorded for primary inclusions hosted by coarse white dolomite-cemented  
477 breccias. On average, these inclusions display higher  $T_h$  and slightly lower salinity than sphalerite-  
478 hosted inclusions in the Rathdowney Trend deposits or prospects and could represent high-  
479 temperature, end-member ore fluids prior to fluid mixing. Pink dolomite ( $D_5$ ) in the Rathdowney  
480 Trend contains similar inclusions to those observed in the same phase at Lisheen and Galmoy but  
481 with a slightly higher modal  $T_h$  range (110-120 °C compared with 90-100 °C and 80-90 °C  
482 respectively). Secondary, low  $T_h$  brine inclusions (28-29 wt% NaCl equivalent), similar to those in pink  
483 dolomite, are common in the Rathdowney Trend prospects.

484 *Courtbrown:* The Courtbrown prospect is located in the southwest Midlands, west of Limerick (Fig.  
485 1). Mineralization occurs as replacement and disseminated styles and is commonly associated with  
486 solution seams (Grennan, 1986). Two-phase fluid inclusions in ore-stage calcite yielded  $T_h$  values  
487 mainly in the range 160-190 °C (Reed and Wallace, 2001). Freezing data were not reported. Although  
488 these results are within the most common range for fluids in the orefield (Table 1), no petrographic

489 evidence for stretching was described, and no size- $T_h$  relationship exists, the authors concluded that  
490 the inclusions must have undergone post-entrapment modification based on inferred overheating to  
491  $\sim 310$  °C (Reed and Wallace, 2001).

492 *Pallas Green*: The Pallas Green prospecting licences are located in the southwest Midlands (Fig. 1).  
493 Five massive sulfide lenses have been discovered in the area: two small zones at Castlegarde and  
494 three larger lenses at Tobermalug, Caherconlish South and Srahane West. This area is currently  
495 undergoing intense exploration and is arguably the most prospective greenfield region in the  
496 orefield. Mineralization at Castlegarde comprises a variety of replacement, breccia and cavity-fill  
497 styles. Early marcasite and pyrite, which may form massive intervals in drillcore, partly replace early  
498 calcite cements and Waulsortian hostrock clasts. Sphalerite is often very finely color-banded, partly  
499 replaces earlier Fe sulfides, and contains later euhedral and dendritic galena (Crowther and  
500 Wilkinson, unpublished report to the Noranda-Minco joint venture, 2002).

501 Two-phase fluid inclusions were analyzed in calcite that infills sulfide-lined vugs and is sometimes  
502 replaced by sulfides. The majority of  $T_h$  values ranged from 132-181 °C with a mode of 150-160 °C.  
503 Salinities varied from 16.1 to 4.3 wt% NaCl at approximately constant  $T_h$  possibly indicative of a  
504 dilution trend.

505

#### 506 *Regional Carbonate Cements*

507 Fluid inclusion studies on cement phases within the Lower Carboniferous host rock sequence  
508 began in the early 1990's. However, a clear picture of the relationship between cementation stages  
509 and hydrothermal events did not begin to emerge until more detailed fluid inclusion studies were  
510 carried out on exploration drillcore through the late 1990's (Wilkinson, unpublished data, 1996-2000)  
511 and a regional study of the Lower Carboniferous cements and their associated fluid inclusion  
512 populations was begun (Gregg et al., 2001; Johnson et al., 2001, 2009).

513 *Fine replacive dolomite ( $D_{1a}$ )*: Reliable fluid inclusion data have not been obtained from the early  
514 (pre-ore) diagenetic planar dolomite (Fig. 2) due to its fine grain size. Based on textural and isotopic  
515 constraints, this has been interpreted as an early, seawater-related diagenetic product (Gregg et al.,  
516 2001).

517 *Coarse white dolomite ( $D_{1b}$ )*: A few  $T_h$  data were reported from aqueous liquid-vapour inclusions  
518 in coarse white "regional" dolomite (Fig. 2) in the 1990's (Allan et al., 1992; Eyre, 1998) suggesting  
519 precipitation temperatures up to 233 °C and apparently ruling out a simple diagenetic origin (cf.  
520 Hitzman, 1995; Hitzman et al., 1998). Subsequent work on similar, non-planar replacement dolomite  
521 yielded rare data from two-phase aqueous inclusions with  $T_h$  values of 170-200 °C and salinities of  
522  $\sim 2$ -15 wt% NaCl equivalent (fluid "Type 2": Gregg et al., 2001). It was concluded that this cement  
523 probably originated via partial neomorphic recrystallization and overgrowth of the early planar

524 dolomite in the presence of late diagenetic or hydrothermal fluids. More recent studies have  
525 reported the common occurrence of aqueous liquid-vapour fluid inclusions, distributed along growth  
526 zones, in Waulsortian-hosted samples of coarse white dolomite from throughout the Midlands  
527 (Wilkinson, unpublished data; Wilkinson, 2003).  $T_h$  data are in the range 140-240 °C with salinities of  
528 10-15 wt% NaCl equivalent, identical to the majority of hydrothermal fluids observed in the deposits  
529 (Table 1).

530 *White dolomite-cemented breccias:* Breccias cemented by planar to non-planar white dolomite  
531 (Fig. 2) are similar to the white matrix breccias associated with mineralization (Doyle et al., 1992;  
532 Hitzman et al., 2002; Wilkinson et al., 2005b) in terms of texture, cathodoluminescence and primary  
533 liquid-vapor fluid inclusion properties (Wilkinson, 2003; Table 1). These inclusions have similar  
534 salinities but slightly higher  $T_h$  values than those hosted by coarse white dolomite and some develop  
535 clathrate on cooling, indicative of elevated  $CO_2$ , as previously reported from deposit sphalerite and  
536 Lower Paleozoic-hosted quartz-carbonate veins (Everett et al., 1999a).

537 An unusual dolomite with uncertain paragenetic position has also been studied. This generally  
538 comprises fine- to coarse-grained, planar-subhedral turbid crystals that commonly display a  
539 pearlescent appearance and cream to pinkish color in hand sample. It appears to be replacive in  
540 origin and is texturally similar to the fine replacive regional dolomite (Fig. 2) except for its coarser  
541 grain size. It is often overgrown by translucent dolomite, occasionally with red or brown ferroan  
542 growth bands, that displays weak, non-planar form (Fig. 4B). Late, transparent vug-filling calcite may  
543 be present, possibly equivalent to  $C_6$  (Fig. 2). Primary inclusions in growth bands are common in the  
544 translucent dolomite and these have similar properties to those observed within some of the earlier  
545 turbid dolomite; therefore, they are both thought to have precipitated from the same fluid type.  
546 Average first melting temperatures of -53.2 °C indicate the predominance of NaCl and  $CaCl_2$ . Final ice  
547 melting temperatures are unusually low, ranging from -23.0 to -35.3 °C (Fig. 4B) and, where  
548 observed, hydrohalite melting occurs after ice with a mean temperature of -1.7 °C (Table 1). These  
549 data imply distinctive Ca-rich brine compositions.

550 *Black dolomite:* Breccia samples from Ballinasloe in the west-central Midlands (Fig. 1) yielded the  
551 only fluid inclusion data yet to be acquired from fine planar black dolomite of the type elsewhere  
552 associated with ore in the Waulsortian-hosted deposits (Wilkinson and Earls, 2000; Fig. 2). This  
553 yielded  $T_h$  values of 146-204 °C, salinities of 13.5-19.9 wt% NaCl equivalent and  $T_{m,hyd}$  in a few  
554 inclusions close to -22 °C indicating NaCl-dominant compositions comparable with inferred ore-stage  
555 fluids at Silvermines, Tynagh, Lisheen and Galmoy. The spread in salinity was considered to be due to  
556 mixing of a moderate salinity (~12 wt%), higher temperature fluid with a low temperature brine; this  
557 process induced rapid supersaturation and precipitation of the characteristic dolomite type. Slightly  
558 earlier white to translucent dolomite that formed reaction rims around breccia clasts hosted two-



559 phase inclusions with  $T_h$  values of 144-203 °C and salinities of 10.3-13.5 wt% NaCl equivalent, similar  
560 to coarse white dolomite elsewhere.

561 *Pink dolomite:* Paragenetically late, coarse grained, cream to pink dolomite (Fig. 2), is widely  
562 observed in the Midlands as a replacement, vug- and vein-filling cement phase (e.g., Boast et al.  
563 1981; Andrew 1986; Eyre 1998), and has also been described cutting mineralized veins in the Lower  
564 Paleozoic basement (Everett et al., 1999a). It displays a well-developed saddle morphology and  
565 shows pronounced compositional zoning in CL (Wilkinson, 2003). It commonly occurs as an  
566 overgrowth of earlier coarse white dolomite in vugs and, as a result, may be confused with this  
567 earlier dolomite. Minor sulfides (mainly pyrite, chalcopyrite and sphalerite) are occasionally observed  
568 encrusting pink dolomite crystals which may explain why this dolomite has been interpreted as pre-  
569 ore (Wright et al., 2000). However, where observed in the deposits, it is always post-ore and is  
570 associated with extensive dissolution of sulfides (Boast et al., 1981; Eyre, 1998).

571 The pink dolomite contains two-phase liquid-vapour inclusions with very consistent properties  
572 (Table 1). Homogenization temperatures are mostly in the range 91-137 °C and salinities are 23.7-  
573 24.7 wt% NaCl equivalent. First melting is normally observed below -50 °C indicating significant  $\text{CaCl}_2$ ,  
574 but combined ice and hydrate melting temperatures (average -17.9 °C) indicate that these brines  
575 have  $\text{Na} > \text{Ca}$ .

576 *Other dolomite data:* Gregg et al. (2001), Mulhall (2003) and Johnson et al. (2001, 2009) identified  
577 three main types of fluid in the Midlands based on inclusions hosted by “late diagenetic” saddle  
578 dolomite cements, but the relative timing of the hosting dolomites was not fully resolved. Based on  
579 analogy with known fluids elsewhere in the Midlands it is considered probable that the saddle  
580 dolomite that hosts inclusions homogenizing in the range 100-270 °C and with salinities of 0-17 wt%  
581 NaCl equivalent (“Type 2” and “Type 3” fluids: Gregg et al., 2001) is correlatable with coarse white  
582 and/or white matrix breccia dolomite (Fig. 2), whereas the white to pink saddle dolomite cements  
583 hosting inclusions with  $T_h$  values of 70-120 °C and salinities of 19 to >26 wt% NaCl equivalent are  
584 likely to be equivalent to the late (post-ore) pink dolomite described above. The difficulty in  
585 distinguishing between some of the dolomite types is probably due in part to the development of  
586 epitaxial overgrowths. For the late pink dolomite, its field distinction is largely based on a coloration  
587 that is not always developed. Significantly, the “Type 3” fluid, that has comparable properties to the  
588 ore-forming fluids (Table 1), was not observed in Supra-Waulsortian lithologies (Johnson et al., 2001,  
589 2009), consistent with a principal high-temperature hydrothermal event that predated their  
590 deposition (e.g., Lee and Wilkinson, 2002).

591

592 *Footwall stratigraphy*

593 The first study of fluid flow at greater paleodepths investigated the structural, mineralogical and  
594 isotopic characteristics of vein systems hosted by Lower Paleozoic rocks. This was coupled with fluid  
595 inclusion data to test whether mineralizing fluids had circulated in fracture permeability within this  
596 volcanosedimentary succession (Everett et al., 1999a). Three main vein types were identified that cut  
597 dark grey-green Silurian greywackes, mudstones and sandstones in the southwest Irish Midlands at  
598 locations up to 32 km WSW and 20 km ESE of Silvermines (Fig. 1):

599

- 600 1. Early hematitic calcite-quartz ± pyrite
- 601 2. Quartz-calcite ± sphalerite, galena, chalcopryrite, pyrite, barite
- 602 3. Ankerite-ferroan dolomite-quartz ± sphalerite, pyrite

603

604 Vein types 2 and 3 are associated with weak to locally intense sericite-chlorite-carbonate alteration,  
605 and disseminated pyrite(-carbonate) is observed in the vicinity of well-developed vein systems. Clots  
606 of a distinctive fine-grained pistachio green mineral are commonly observed within Type 2 veins and  
607 along vein margins and more rarely in Type 3 veins. In some cases it is associated with pink dolomite  
608 that cuts both vein types. Microprobe analyses indicate that these comprise phengitic K-mica,  
609 sometimes intimately intergrown with chlorite.

610 The majority of the fluid inclusions observed were of liquid-vapor aqueous type with a minority of  
611 secondary monophasic, liquid-only inclusions. Inclusions within quartz which showed a highly variable  
612 degree of fill from 5 to 75 percent liquid were recorded in one sample – possible evidence for boiling.  
613 Some liquid-vapor and liquid-only inclusions contained trapped solid phases that showed no change  
614 upon heating; these were interpreted to be calcite and K-mica.

615 Inclusions considered to represent the vein-forming fluids in Type 1 veins had low to moderate  
616 salinities (0.2-10.8 wt% NaCl equivalent) and  $T_h$  values from 150-250 °C. Lower temperature (109-  
617 189.9 °C), moderate to high salinity (12.2-23.8) secondary inclusions were also recorded. The origin  
618 of the Type 1 veins is uncertain, although structural relationships are consistent with a Lower  
619 Carboniferous age, and the occurrence of hematite, chlorite and calcite is similar to the early (pre-  
620 sulfide) ironstones and associated hematite-bearing veins reported at several Irish base metal  
621 deposits (Hitzman et al., 1995). However, the fluid properties are also comparable with inclusions  
622 commonly associated with the Caledonian granites in Ireland, interpreted to represent widespread  
623 meteoric circulation subsequent to their emplacement and crystallization (O'Reilly et al., 1997a,b).

624 Primary fluid inclusion data from vein Types 2 and 3 show  $T_h$ -salinity characteristics (123-238 °C,  
625 9.7-20.6 wt% NaCl equivalent) that are comparable with data from Carboniferous-hosted  
626 mineralization (Table 1). In addition, the highest  $T_h$  inclusions hosted by quartz and sphalerite

627 commonly contain CO<sub>2</sub> as noted elsewhere. These fluids are believed to represent ore fluids trapped  
628 en route to potential sites of mineralization.

629

### 630 **Fluid Inclusion Constraints on Fluid Origins and Interactions**

631

632 Although basic microthermometric data provide important constraints on fluid properties and  
633 variability within hydrothermal ore systems (e.g. Wilkinson, 2001), greater insights are provided by  
634 more complete fluid geochemical information. At the first level, this includes interpretation of ice  
635 and hydrate melting temperatures in the NaCl-CaCl<sub>2</sub>-H<sub>2</sub>O system which yields information on trends  
636 in the major cation compositions of the fluids. More detailed geochemical studies, using bulk  
637 methods (crush-leach or decrepitation-linked ICP analysis), have also been carried out in Ireland,  
638 principally to provide constraints on the origin of the ore-forming solutions. The use of laser ablation  
639 ICP-MS for the analysis of individual inclusions is just starting to be applied and is providing  
640 important new data on metal contents (Wilkinson et al., 2009).

641

#### 642 *Na:Ca ratios*

643 In order to interpret fluid inclusion chemistry in chemical systems more complex than NaCl-H<sub>2</sub>O  
644 from microthermometric data it is necessary to observe additional phase changes, such as hydrate  
645 melting. However, in studies of the Irish orefield this phase transition has been reported only rarely  
646 (Samson and Russell, 1987; Banks and Russell, 1992; Eyre, 1998). These results indicated that fluids  
647 generally had Na numbers (Na#: NaCl/[NaCl+CaCl<sub>2</sub>]) greater than 0.5. Based on crush-leach data,  
648 Samson and Russell (1987) suggested that the moderate salinity ore fluids had high Na# and that two  
649 brine types existed, one with high Na# and one with low Na#.

650 Here, new data are presented from basement-hosted veins, regional carbonates, deposits  
651 (Silvermines) and prospects (Keel and Castlegarde). Excluding three outliers below -30 °C (probably  
652 erroneous observation), T<sub>m,hyd</sub> ranges from to -29.0°C to +1.1 °C, but is mostly between -22 and -24  
653 °C (Table 1). Modelling ice and hydrate melting in the NaCl-CaCl<sub>2</sub>-H<sub>2</sub>O system (Naden, 1996) gives  
654 Na# mostly in the range of 0.66-0.95 for basement-hosted veins, 0.42-0.88 for regional carbonates,  
655 and 0.61-0.92 for deposits and prospects. The uncertainty for careful measurement of T<sub>m,hyd</sub> is ±0.2  
656 °C and for ice melting ±0.1 °C which translates into a modeled uncertainty of +0.03/-0.01 in Na# and  
657 ±0.1 wt% in total salinity (wt% NaCl+CaCl<sub>2</sub> equivalent). The degree of uncertainty due to the presence  
658 of other cations or anions in the fluids cannot be assessed. Plotting Na# as a function of total salinity  
659 allows possible end-member fluids and mixing relationships to be identified (Fig. 5).

660 The regional carbonate data suggest that two brine compositions exist with Na# of ~0.75 (25 wt%  
661 salinity; Type B<sub>1</sub>) and Na# ~0.60 (28 wt% salinity; Type B<sub>2</sub>), in agreement with Samson and Russell

662 (1987). Type B<sub>1</sub> is principally associated with pink dolomite and has compositions similar to Triassic,  
663 red-bed derived, evaporitic brines recorded in Southwest England (Gleeson et al., 2001; Stoffell et al.,  
664 2004). It corresponds to the “Group 3” calcite-hosted inclusions of Banks and Russell (1992) at  
665 Tynagh. Type B<sub>2</sub> is associated with cream to pink, turbid, replacement dolomite or the more  
666 transparent dolomite that overgrows it. A third, calcic brine (B<sub>3</sub>), sometimes spatially associated with  
667 the B<sub>2</sub> brines (Fig. 4), is inferred from inclusions that display very low ice melting temperatures  
668 (typically around -33 °C). Although hydrate melting generally was not observed, the topology of the  
669 NaCl-CaCl<sub>2</sub>-H<sub>2</sub>O phase diagram indicates variably Ca-rich fluid compositions with Na# between ~0.2  
670 and 0.6. These fluids have been found associated with Supra-Waulsortian dolomitized shelf  
671 limestones to the west of Ballinasloe and younger (up to Holkerian or early Asbian) shelf limestones  
672 southwest of Stradbally in Co. Laois (Fig. 1) indicating that they were present (although not  
673 necessarily exclusively) post-mineralization.

674 Results for moderate salinity fluids in basement-hosted veins (LP<sub>1</sub>) indicate relatively high Na#  
675 (0.7-0.9), typical for ore fluids from Silvermines (Samson and Russell, 1987). Basement-hosted  
676 sphalerite typically displays average Na# ~0.75 at the lower end of this range. The variation in Na# as  
677 a function of total salinity could reflect LP<sub>1</sub>-B<sub>2</sub> mixing in the upper parts of the basement immediately  
678 beneath the basinal succession or salinity-dependent siliciclastic buffering of fluid composition, with  
679 lower Na/Ca characterizing slightly higher salinity fluids (e.g., Yardley, 2005). However, there are  
680 insufficient data to properly constrain these possibilities at present.

681 Deposit-hosted sphalerite trapped fluids of distinct composition that are of relatively low salinity  
682 but more calcic than the LP<sub>1</sub> fluids. It is therefore possible that the actual ore-forming fluids were of  
683 somewhat different composition (particularly in their metal budget) to at least some of the fluids  
684 trapped in feeder veins in the basement as has recently been suggested on the basis of LA-ICP-MS  
685 analyses of inclusions (Wilkinson et al., 2009). The more calcic compositions could be indicative of  
686 greater degrees of fluid-rock interaction (see below). Alternatively, it may be that fluid compositions  
687 were shifted toward more calcic compositions during ore deposition. Sphalerite precipitation as a  
688 result of fluid mixing generates acid that can result in carbonate dissolution and consequent Ca  
689 (+Mg) enrichment in the fluid according to reactions such as:

690



692

693 This type of reaction is supported by abundant textural evidence for delicate replacement of  
694 different carbonate grain types by sulfides, as has been described from Lisheen (Wilkinson et al.,  
695 2005b). A third possibility is that ore formation resulted from mixing between fluids of LP<sub>1</sub> type and

696 the calcic B<sub>3</sub> brines (Fig. 5). However, this is thought to be unlikely given the young (probably post-  
697 ore) age of the B<sub>3</sub> brines identified to date.

698

#### 699 *Major element chemistry*

700 Bulk fluid inclusion analyses on quartz from basement-hosted vein samples (Everett et al., 1999a)  
701 showed that LP<sub>1</sub> fluids had Na>Ca≥K and were Mg-poor. These compositions are comparable with  
702 experimental data on fluids equilibrated with greywackes at temperatures of 200-350 °C, consistent  
703 with derivation of mineralizing fluids from a Lower Paleozoic-equilibrated fluid reservoir. Na# were in  
704 the range 0.88-0.94, consistent with the microthermometry-derived values reported here. Na-K-Ca  
705 (Fournier & Truesdell, 1973) and K-Na and K-Mg alkali thermometers (Giggenbach, 1988) can be  
706 applied because the mineralogy of the Lower Paleozoic succession (quartz, albite, K-feldspar,  
707 muscovite, chlorite, illite, minor carbonate, trace sulfides) is similar to that in the geothermal  
708 reservoirs from which the thermometers are calibrated. These geothermometers gave equilibration  
709 temperatures (158-219 °C) not significantly different to T<sub>h</sub> values suggesting that the inclusions were  
710 trapped under pressures only slightly above saturated vapor pressure, indicating a relatively shallow  
711 depth of vein formation. In terms of the detail of flow patterns and the relationship between these  
712 feeder vein localities and the deposits, it may be important that these temperatures are lower than  
713 many of the estimates for fluid temperatures in the ore deposits (Table 1).

714

#### 715 *Halogen geochemistry*

716 The first halogen analyses of Irish fluids were presented by Everett (1999), Everett et al. (1999b)  
717 and Gleeson et al. (1999), and were further expanded by Banks et al. (2002), Wilkinson et al. (2005a)  
718 and Johnson et al. (2009). Although the uncertainty in these measurements is difficult to constrain,  
719 different fluid types can be identified based on significant differences in halogen and major element  
720 ratios and/or the restriction of particular signatures to specific paragenetic stages or geographic  
721 locations.

722 Lower Paleozoic-hosted vein samples contain fluids that fall into two groups: Type LP<sub>1a</sub> have Cl/Br  
723 molar ratios (559-825) that are similar to seawater, interpreted as being produced by partial  
724 evaporation of seawater to an evaporation ratio of ~4x to ~7x (evaporation ratio = mass of water in  
725 seawater/mass of water in evaporated brine) prior to circulation into the basement (Wilkinson et al.,  
726 2005a). Type LP<sub>1b</sub> fluids are slightly less saline but have Cl/Br values below seawater (375-553); these  
727 were interpreted to represent strongly evaporated bitters (evaporation ratio up to 25x), relatively  
728 enriched in Br, that had subsequently been diluted by either seawater, evaporated seawater or  
729 meteoric water (Fig. 6A). Mixing curves show that the data are consistent with mixtures containing  
730 ~5-20% brine (by mass) and ~80-95% evaporated seawater although other possibilities cannot be

731 excluded at present. The relatively narrow salinity range displayed by the LP<sub>1b</sub> fluids (Everett et al.,  
732 1999a) implies homogenization of these putative mixtures prior to trapping but it is uncertain when  
733 this mixing occurred: prior to recharge, during flow within basement rocks, or close to the  
734 paleosurface around the time of mineralization. Hydrogen and oxygen isotope data (see below) are  
735 consistent with a model involving mixing of uninteracted brines (relatively near to the paleosurface)  
736 with strongly interacted LP<sub>1</sub>-type fluids to form the LP<sub>1b</sub> fluids.

737 Results from deposit-hosted samples show that ore fluids from Silvermines are similar to LP<sub>1a</sub>  
738 whereas those from Tynagh are shifted to slightly more Br-rich compositions, closer to LP<sub>1b</sub>. Tentative  
739 modeling indicates that mixing between Br-enriched brines (<20%) and LP<sub>1</sub> fluids (evolved partially  
740 evaporated seawater; >80%) can produce most of the range in Cl-Br compositions observed in the  
741 Irish ore fluids (Fig. 6A) although it is possible that some of the spread is an artefact due to analysis of  
742 inhomogeneous inclusion populations. Nonetheless, the data are consistent with trapping of  
743 mixtures of high temperature fluids and brines at the ore depositional site, a process that has been  
744 invoked as a key ore-forming mechanism (e.g. Anderson et al., 1998; Blakeman et al., 2002; Hitzman  
745 et al., 2003; Wilkinson et al., 2005a, 2005b).

746 Combining exchangeable cation data with the conservative halogens allows processes undergone  
747 by these seawater-derived fluids during crustal interaction to be explored. A plot of Cl/Br vs. Na/Br  
748 (Fig. 6B) shows that all deposit and Lower Paleozoic basement-hosted vein data lie close to or above  
749 the seawater evaporation trajectory (SET), best explained by loss of Na from fluids initially lying at  
750 various points along the SET. Fluids from Silvermines appear to be more exchanged than those from  
751 Tynagh, possibly accounted for by a greater degree of water-rock interaction, which could explain  
752 the greater metal endowment of the Silvermines system. Both deposits appear to have formed from  
753 more exchanged fluids (subsequently referred to as LP<sub>2</sub>) than the Lower Paleozoic-hosted veins,  
754 suggesting that the feeder veins (sampled lateral to the deposits) represent different, less basement-  
755 interacted, parts of the flow system. The samples from Birdhill and Latteragh (closer to Silvermines;  
756 Fig. 1) generally display greater degrees of Na loss than those from Fantane and Ballycar (Fig. 6B),  
757 consistent with a convective type of flow pattern.

758 An equivalent plot but involving Ca (Fig. 6C) shows that there is very strong enrichment in Ca in  
759 the Lower Paleozoic-hosted vein fluids relative to evaporated seawater. Unfortunately, no  
760 comparable data for deposit-hosted inclusions exist. The exchange of Ca<sup>2+</sup> for 2Na<sup>+</sup>, most commonly  
761 mediated by reactions involving plagioclase, is a common process in crustal fluid-rock interactions  
762 and is related to temperature and fluid salinity (Yardley, 2005). Ca is most enriched in samples from  
763 the Birdhill and Latteragh localities supporting greater degrees of exchange in the genesis of these  
764 fluids, consistent with the Na data. However, consideration of the cation balance shows that the Ca  
765 gain in the LP<sub>1</sub> fluids is not matched by twice as great a loss (in molar terms) in Na so that an

766 additional source of Ca is required. One possibility is that Ca was acquired from the Carboniferous  
767 sequence as a result of Mg-Ca exchange dolomitization in downflow zones:

768



770

771 Some of the pre-mineralization, seawater-related dolomitization observed ( $D_{1a}$ ) could have been  
772 formed in this way and the process may also have been responsible for some of the Mg depletion  
773 noted in the  $LP_1$  fluids, although this can also be attributed to Mg-smectite and chlorite formation in  
774 the basement rocks (see below).

775 Microthermometric data suggest that deposit sphalerite-hosted ore fluids ( $LP_2$ ) are even more Ca-  
776 rich than  $LP_1$  fluids (Fig. 5) and this is supported by recent LA-ICP-MS analyses (Wilkinson et al.,  
777 2009). This is consistent with greater degrees of basement exchange in their production although, as  
778 noted earlier, the possibility of local Ca increase due to carbonate dissolution at the site of ore  
779 formation cannot be excluded.

780

#### 781 *Minor and trace element chemistry*

782 Plotting the minor and trace element chemistry of the  $LP_1$  fluids normalized to their inferred  
783 evaporated seawater precursor illustrates the Li enrichment, strong Mg depletion, and broad  
784 increase in the transition metals and lithophile elements (Sr, Ba, Pb), that has occurred during crustal  
785 interaction (Fig. 7). Similar changes are observed in modern seawater-dominated submarine  
786 hydrothermal fluids interacting with ocean basalts, but with a lack of such strong enrichment in  
787 elements concentrated in felsic crust such as Ba or Pb.

788 Lithium concentrations in  $LP_1$  fluids are in the range 55-164 ppm (Everett et al., unpublished;  
789 Wilkinson et al., 2005a), overlapping with, but generally lower than, the 86-503 ppm obtained by  
790 crush-leach analysis from Silvermines and Tynagh ore-stage samples (Banks et al., 2002). All these  
791 values are elevated significantly above evaporated seawater concentrations. Enrichment is most  
792 likely due to interaction with basement rocks that typically contain 30-60 ppm Li (Crowther, 2007).

793 Magnesium concentrations in  $LP_1$  fluids are in the range 30-310 ppm and are very depleted (Fig.  
794 7), typical of seawater-derived fluids that have undergone low temperature exchange with silicate  
795 rocks and/or have been involved in dolomitization. Thus, the Mg data, like Na, can be explained by  
796 exchange for Ca during fluid infiltration.

797 Barium is strongly enriched in  $LP_1$  fluids, such as at Fantane (mean 930 ppm; Wilkinson et al.,  
798 2005a), even in the absence of significant base metals. It could be acquired by fluids from trace  
799 barite or barian feldspar during basement interaction, but only once fluids were depleted in sulfate  
800 either by anhydrite precipitation or reduction.

801 Bulk data suggest that ore metal concentrations are low in LP<sub>1</sub> fluids (2-33 ppm Zn, 11-68 ppm Pb;  
802 Everett et al., unpublished; Wilkinson et al., 2005a) and are highest in the most interacted fluids  
803 (based on Na/Br systematics) at Birdhill and Latteragh. This contrasts markedly with recent analyses  
804 of sphalerite-hosted inclusions from Silvermines that display one to two orders of magnitude higher  
805 Pb concentrations (Wilkinson et al., 2009). Such high metal contents appear to suggest that unusually  
806 efficient metal extraction was responsible for production of the LP<sub>2</sub> fluids that went on to form ore,  
807 potentially linked to the greater degrees of water-rock interaction suggested above.

808

#### 809 *Oxygen and hydrogen isotopes*

810 Fluid  $\delta D$  (obtained by direct measurement of fluid inclusions) and calculated fluid  $\delta^{18}O$  values  
811 (based on mineral compositions and mineral-water fractionation factors) from ore-stage samples at  
812 Silvermines were interpreted to reflect equilibration of seawater-derived fluids with the Lower  
813 Paleozoic sequence (Samson and Russell, 1987). Similar data from Lower Paleozoic-hosted feeder  
814 veins (Everett et al., 1999b) suggested mineralizing solutions with  $\delta^{18}O_{H_2O} = 2.4-9.0\text{‰}$  and  $\delta D = -24$  to -  
815  $55\text{‰}$ , overlapping with the Silvermines orefluids. This is supporting evidence for Lower Paleozoic  
816 flow of the ore-forming solutions, although the generally lower  $\delta D$  of the Silvermines fluids is  
817 noteworthy.

818 Modeling of these data using the new constraints on fluid origins discussed above shows that the  
819 measured compositions cannot be produced by equilibration of seawater or evaporated seawater  
820 with inferred Lower Paleozoic rock compositions, even at low water/rock ratios (Fig. 8). Utilising a  
821 possibly depleted Carboniferous seawater precursor ( $\delta^{18}O = -3\text{‰}$ ; Veizer et al., 1999) has negligible  
822 effect because fully-equilibrated fluids at low water/rock ratios are essentially buffered by the rock  
823 composition. The discrepancy requires involvement of an unexchanged fluid with much lower  $\delta D$ ,  
824 lower fluid-rock fractionation factors for hydrogen and/or lower  $\delta D$  of the rocks involved. The  
825 observation that low temperature brine inclusions trapped in barite at Silvermines are characterized  
826 by low  $\delta D$  values ( $-41.4$  to  $-54.6\text{‰}$ ; Samson and Russell, 1987) suggests that a D-depleted shallow  
827 brine may have existed and mixing between this and exchanged evaporated seawater could explain  
828 the relatively D-depleted LP<sub>1</sub> fluid data and some of the ore fluid compositions (Fig. 8). A possible  
829 explanation for the depleted brine signature is bacterial fractionation of hydrogen isotopes at the  
830 seafloor (Samson and Russell, 1987); however, it can also be reproduced by shifting the seawater  
831 evaporation trajectory to lower  $\delta^{18}O$  and  $\delta D$  values and assuming a depleted Carboniferous seawater  
832 precursor (Fig. 8). Thus, the low  $\delta D$  signature could be merely a product of evaporation past halite  
833 precipitation (cf. Knauth and Beeunas, 1985).



834 The isotopic compositions of the bulk of the Silvermines ore fluids (which tend to have higher  $T_h$   
835 values and lower salinities than most  $LP_1$  fluids) cannot be explained by brine- $LP_1$  mixing in the ore-  
836 forming environment (Fig. 8) and appear to require a greater hydrogen isotope shift during fluid-rock  
837 interaction. The involvement of D-depleted lithologies at greater depth cannot be tested although  
838 this would be consistent with the higher fluid temperatures suggested by higher  $\delta^{18}O$  values and  
839 generally higher  $T_h$  values. Interaction with mafic rocks ( $\delta D$  -70 to -105 ‰; Agrinier et al., 1995),  
840 Caledonian granite or the Precambrian crystalline basement that may have undergone earlier  
841 deuteritic alteration are all possibilities.

842

843

## Discussion and Implications

844

### *Regional fluid evolution*

845 Fluid inclusion data, coupled with stable and radiogenic isotope systematics, describe a basinal  
846 system in which widespread mobilization of hydrothermal fluids led to progressive overprinting of  
847 normal, early diagenetic processes and localized convergence of a number of factors toward ore-  
848 forming conditions. Fluid chemistry suggests that some of the early dolomitization ( $D_{1a}$ ; Fig. 2) could  
849 have formed from “normal” evaporated seawater that subsequently penetrated the basement and  
850 evolved into interacted but unfertile solutions. Regionally-developed, coarse white dolomite cements  
851 ( $D_{1b}$ ) then formed above fault-focused plumes of these evolved solutions, as they became thermally  
852 buoyant and migrated back toward the surface. The coarse white dolomite is thus interpreted to  
853 reflect a slightly lower temperature and spatially more extensive manifestation of the hydrothermal  
854 system that was ultimately responsible for the formation of the ore deposits (Wilkinson, 2003).

855 Increased focusing and greater penetration depth are inferred to have led to the local generation  
856 of higher temperature, more exchanged, highly metalliferous fluids. It was only where these  $LP_2$   
857 fluids returned to the near seafloor environment and mixed with sulfidic brines that economic  
858 mineralization was formed, accompanied by hydrothermal dolomite ( $D_2$ ,  $D_3$ ). Continued flow of these  
859 fluids after the main mineralizing event(s), with brines excluded from the ore systems perhaps by the  
860 deposition of impermeable capping sequences (e.g., Calp Limestone over the Waulsortian; Upper  
861 Dark Limestones over the Navan Group), led to overprinting of ore by late stage veins in some of the  
862 deposits ( $D_4$ ,  $C_4$ ).

863 The late pink dolomite ( $D_5$ ) is a distinct, post-ore marker that has been interpreted in terms of a  
864 post-ore brine migration, probably related to the onset of Variscan compressional tectonism in the  
865 mid- to late Carboniferous (Andrew, 1986; Wilkinson, 2003; Wilkinson et al., 2003). Thus, the onset  
866 of compression in the Midlands Basin is considered to have been the principal tectonic control that  
867 switched off convective fluid circulation.  
868

869

870 *Regional variations in fluid properties*

871 The compilation of microthermometric data presented resolves some trends not previously  
872 recognized. Plotting principal modal  $T_h$  and salinity data from each locality (Fig. 9) shows that there is  
873 a regional pattern, with lower  $T_h$  and/or lower salinity fluids predominant in the north and western  
874 Midlands and higher  $T_h$ , higher salinity fluids in the south and east. This division corresponds broadly  
875 to the position of the Iapetus Suture Zone (Fig. 1) and it is proposed that this marks a major  
876 discontinuity between flow systems operating in the two halves of the Midlands Basin. Evidence for a  
877 contrast in the chemical composition of fluids in the northern Midlands compared with the south  
878 was previously suggested by Wilkinson et al. (2007) based on a preliminary regional LA-ICP-MS study  
879 of fluid inclusions in feeder veins. This showed that Zn:Pb ratios and Zn contents were significantly  
880 higher in the northern Midlands localities investigated, possibly related to a greater volcanic  
881 contribution in the Lower Paleozoic basement to the north of the Iapetus Suture. The generally lower  
882  $T_h$  values in the northern domain is presumed to reflect a shallower circulation system, possibly  
883 limited by a thinner Lower Paleozoic sequence underlain by relatively impermeable Dalradian or  
884 Lewisian metamorphic rocks. Nonetheless, some interaction with the crystalline basement in the  
885 north has been suggested based on Nd isotope analyses of hydrothermal carbonates (Walshaw et al.,  
886 2006).

887 Higher temperatures, particularly in the southwest, are consistent with the lower Zn:Pb ratios in  
888 these fluids and higher  $\delta^{18}\text{O}$  values. At Tynagh and Silvermines, there is evidence that submarine  
889 warm springs developed (Banks, 1985; Boyce et al., 2003; Wilkinson et al., 2003, 2005a) perhaps  
890 because these rising fluids were more buoyant due to their higher temperatures and lower salinities  
891 and were consequently able to punch through cool, dense porewater bodies resident in the shallow  
892 sediments to reach the seafloor. Elsewhere (e.g. Lisheen, Galmoy, Navan), dense shallow brines may  
893 have impeded venting with possible late stage exhalation at Navan linked to unroofing of the deposit  
894 due to major tectonic instability and submarine gravity sliding during development of the Boulder  
895 Conglomerate (Ashton et al., 1986).

896 In terms of their  $T_h$ -salinity properties, the fluids associated with the MVT deposits are distinct  
897 and do not clearly fit the broader regional pattern (Fig. 9). It is noteworthy that the principal area in  
898 which these deposits are observed is spatially associated with a low in the regional vitrinite/CAI  
899 maturity data. This relationship suggests that this region has not undergone the same subsidence  
900 and higher temperature fluid flow history as much of the rest of the Midlands and is consequently  
901 suggested to be not prospective for true Irish-type deposits (*sensu* Wilkinson, 2003).

902

903 *Brine origins*

904 Seawater evaporation to varying degrees played a key role in the generation of ore fluids for the  
905 Irish Zn-Pb deposits. The principal ore fluids were produced from partially evaporated seawater; there  
906 is no evidence for the involvement of brines produced by halite dissolution as would probably be  
907 required in the lateral flow models driven by Variscan topographic relief (e.g., Hitzman and Beaty,  
908 1996). An interesting question is why only these partially evaporated fluids appear to have circulated  
909 to depth. It could be due to the paleogeography, with recharge areas only tapping marine waters  
910 from partially restricted sub-basins and not from areas of high evaporation (Fig. 10). A complex  
911 paleogeographic control on brine evolution has been recognized in studies of recent intracratonic  
912 marine basins such as the Dead Sea (Klein-BenDavid et al., 2004). Alternatively, more strongly  
913 evaporated brines may also have circulated into the basement but were too dense to undergo return  
914 buoyant flow to the near-surface.

915 More strongly evaporated brines were widespread, but these are only recognized in the Lower  
916 Carboniferous succession, with the exception of the small component inferred to be present in the  
917 LP<sub>1b</sub> fluids. Three brine types have been identified, all enriched in Ca: (B<sub>1</sub>) relatively high Na# (~0.8)  
918 brines associated with pink dolomite; (B<sub>2</sub>) more saline brines with elevated Ca (Na# ~0.5) associated  
919 with pervasive dolomitization; and more calcic brines (Na# ~0.6-0.2), associated with dolomitization  
920 of shelf limestones. Evaporation of modern seawater only produces very low Ca brines due to the  
921 precipitation of gypsum and an excess of SO<sub>4</sub><sup>2-</sup> over Ca<sup>2+</sup>. The observed variable enrichments in Ca are  
922 therefore most likely due to Ca gain, possibly via gypsum dissolution and, probably more likely, Ca-  
923 Mg exchange dolomitization. Mole-for-mole replacement of Ca by Mg results in net volume  
924 reduction ( $\Delta V = -9.74 \text{ cm}^3 \text{ mol}^{-1}$ ; -13%), consistent with the observation of increasing porosity and  
925 development of coarse, euhedral saddle dolomite during progressive dolomitization. Similar fluid-  
926 rock interactions have been suggested for the origin of Ca chloride brines in the Dead Sea Rift (e.g.  
927 Stein et al., 2000).

928

#### 929 *Role of fluid mixing*

930 In Ireland, ore formed at the interface between deeply-circulating and shallow, diagenetic flow  
931 systems (e.g. Wilkinson et al., 2005a) within carbonate host rocks, with mixing being an important  
932 process that allowed low-sulfur, metal-rich fluids to saturate with sulfides and at the same time  
933 generate porosity for sulfide deposition. However, fluid inclusion data suggest that mixing also  
934 occurred in other parts of the flow system that, in combination with the variety of fluid types  
935 potentially involved (seawater, variably evaporated seawater, exchanged variably evaporated  
936 seawater, bittern brines), resulted in significant complexity in fluid chemistry. In the Lower Paleozoic  
937 basement there is evidence for mixing of Br-enriched brine with partially evaporated, extensively  
938 exchanged seawater as the latter fluids ascended toward the paleoseafloor. The rare occurrence of

939 barite in Lower Paleozoic-hosted veins with a Carboniferous seawater sulfate signature (Everett,  
940 1999), pyrite with low (ore-like)  $\delta^{34}\text{S}$  values, and variations in Na# in fluid inclusions are consistent  
941 with minor LP<sub>1</sub>-brine mixing within at least the upper parts of the basement sequence.

942 Mixing of LP<sub>2</sub> fluids with brines in the ore-forming environment appears to have been an  
943 important depositional mechanism and the halogen data suggest that Br-enriched bittern brines  
944 were involved. These brines must have become enriched in reduced sulfur by bacteriogenic  
945 reduction (e.g. Boyce et al., 1983; Caulfield et al., 1986) prior to mixing. It is suggested that the  
946 development of submarine hot springs and/or seeps above major hydrothermal plumes resulted in  
947 the local development of chemosynthetic faunal communities including abundant sulfate-reducing  
948 bacteria. These bacterial blooms could have concentrated H<sub>2</sub>S in brines trapped in seafloor  
949 depressions and in underlying lithologies proximal to hydrothermal upflow zones. In the Waulsortian-  
950 hosted deposits, these sulfidic brines could have been resident within permeable Waulsortian that  
951 had been previously dolomitized (e.g. Lisheen, Galmoy; Wilkinson et al., 2005b) or in sedimentary  
952 slump breccias in undolomitized Waulsortian (e.g. Silvermines; Lee and Wilkinson, 2002), perched on  
953 the relatively impermeable underlying argillaceous limestones. Mixing along the interface between  
954 such brine lenses and upwelling LP<sub>2</sub> fluids is consistent with the observation that the base of massive  
955 sulfide is often planar, horizontal and commonly transgresses stratigraphy. Furthermore, the contact  
956 between hydrothermal black dolomite cemented breccias (formed at the mixing interface) and  
957 overlying white matrix breccias (cement precipitated from largely unmodified LP<sub>2</sub> fluids) is  
958 subhorizontal and sharp to gradational over a few meters (Hitzman et al., 2002; Lee and Wilkinson,  
959 2002; Fusciardi et al., 2003).

960 Fluid inclusion data show that, generally, hydrothermal dolomite was precipitated at the highest  
961 temperatures, probably during the first increments of fluid mixing. The lack of Mg in the LP fluids  
962 indicates that mixing with unexchanged, Mg-rich brines is likely to be essential for extensive dolomite  
963 development in areas where pre-existing diagenetic dolomite was not abundant (e.g., Silvermines:  
964 Lee and Wilkinson, 2002). In the south and east Midlands, where early pervasive dolomitization of  
965 the Waulsortian had occurred (Hitzman, 1995), local recrystallization could have supplied some of  
966 the required Mg.

967 Across the orefield, sphalerite-hosted inclusions tend to form relatively tight clusters of data from  
968 individual samples and be polymodal in terms of salinity. The reason for this is uncertain although it  
969 is suggested that the more crystalline sphalerite samples amenable to inclusion analysis may  
970 represent pockets of mixed fluid that precipitated sphalerite during cooling in the waning stages of  
971 individual pulses of hydrothermal fluid ingress. Finer-grained sphalerite types probably precipitated  
972 over a greater part of any mixing interval but the fluid inclusion record of this is only (partly)  
973 preserved in the coexisting gangue. The salinity modes observed may reflect different degrees of

974 mixing but the occurrence of comparable modes in different deposits as well as in basement-hosted  
975 veins (Table 1; Wilkinson et al., 2009) suggests that infiltration of LP fluids of varying salinity and  
976 composition occurred at different times as well as in space. The majority of sphalerite in the  
977 Waulsortian-hosted systems appears to be associated with the more saline mode(s), suggesting that  
978 this (presumably more highly evaporated) interacted seawater was particularly important for ore  
979 formation (Wilkinson et al., 2009).

980 Calcite appears to have been more commonly precipitated during extensive mixing and at lower  
981 temperatures, although some high temperature, unmixed, fluids are responsible for the formation of  
982 calcite feeder veins in some of the deposit footwalls (e.g., Silvermines: Lee and Wilkinson, 2002).

983 At Lisheen, Galmoy, Silvermines (Cooleen Zone), Castlegarde and Keel, a trend toward more  
984 dilute, lower  $T_h$  inclusions has been recognized, consistent with mixing between LP fluids and low  
985 temperature seawater. It is perhaps not surprising that this is observed given the inferred near-  
986 seafloor environment of ore-formation. Evidence from Silvermines suggests that such mixing tends  
987 to be restricted to the margins of the system, outside the region of brine influence. It is suggested  
988 that upwelling orefluids may have been deflected around a dense brine lens, mixing along the  
989 interface with brine and then being diluted by normal seawater along the margins (Fig. 10). Although  
990 seawater mixing does appear to be capable of driving fluids to sulfide saturation (presumably via  
991 cooling and decreased ligand concentration), it is not thought to be favourable for extensive sulfide  
992 deposition due to the limited sulfur supply in the LP fluids. The predominance of deep, hydrothermal  
993 sulfur in these zones is confirmed by the high ( $>0$ )  $\delta^{34}\text{S}$  values observed in the subeconomic Cooleen  
994 Zone at Silvermines (Lee, 2002).

995 The subeconomic prospects generally appear to show a restricted salinity range, being dominated  
996 by LP fluids that vary widely in temperature between localities. At present, it is not known if the  
997 prospects formed from LP fluids with less ( $\text{LP}_1$ ) or more ( $\text{LP}_2$ ) exchanged character. Dilution trends  
998 are observed in some of the prospects (e.g., Castlegarde, Cooleen, Keel), but the brine mixing trends  
999 that appear to be consistently observed in the ore deposits are weak or absent. Thus, LP-brine mixing  
1000 is one of the key factors that appears to be missing from the subeconomic systems. The low  
1001 temperature, possibly slightly younger, MVT deposits show some evidence of mixing but lack the  
1002 elevated temperatures that may be required for significant metal solubilization and show little  
1003 evidence of the bacteriogenic sulfide trap, being typified by positive  $\delta^{34}\text{S}$  values (Dixon, 1990).  
1004 Cooling, neutralization due to extensive retrograde carbonate dissolution, and inorganic sulfate  
1005 reduction are suggested as the controls of sulfide deposition from these late, cool, LP-type fluids that  
1006 are interpreted to reflect the waning phase of the convective flow system.

1007 The formation of economic mineralization in Ireland appears to reflect the coincidence of high  
1008 temperature reaction zones in the basement, brine-producing footwalls, and hangingwall structural-

1009 stratigraphic traps, with bacterial blooms linked to upwelling plumes of hydrothermal fluids. The ore  
1010 deposits can therefore be viewed as products of self-organizing systems – with a first-order structural  
1011 control – that locally converged on ore-forming conditions. Understanding the basement structural  
1012 architecture will therefore be critical for predicting new deposits.

1013

#### 1014 *Wider implications*

1015 The Irish hydrothermal system shares much of the variety and complexity observed in other  
1016 intracratonic basin-hosted Zn-Pb(-Ba) ore districts. This includes the coexistence of contrasting styles  
1017 of mineralization that are typically observed in the more distal and platform-marginal parts of the  
1018 basinal environment (Sangster, 1990). In Ireland, true Irish-type (carbonate-hosted, stratiform-  
1019 stratabound, massive sulfide replacement ore deposits) and MVT deposits are linked by the same  
1020 type of fluids, but the MVT deposits display distinct morphologies and chemical characteristics that  
1021 are related to their likely younger age, lower temperature of formation, and lack of a bacteriogenic  
1022 sulfide trap. Specific characteristics include: non-stratiform breccia geometry, crustiform clast  
1023 coatings, high Zn/Pb, dendritic galena, presence of melnikovite, abundance of marcasite-calcite,  
1024 finely banded colloform sphalerite, and pale crystalline sphalerite. Higher temperature (Irish-type)  
1025 indicators include: stratiform sulfide and (where present) breccia body geometry, massive sulfide  
1026 texture, high Ni and Cd, low Zn/Pb, dark crystalline sphalerite, chalcopyrite, tennantite and other  
1027 sulfosalts.

1028 The Irish-type ore deposits can be viewed as intermediate between classic shale-hosted, deeper  
1029 water Sedex deposits and platform carbonate-hosted MVT deposits in that they formed in a ramp  
1030 environment beneath water depths of up to several hundred meters; they formed at around the  
1031 time of host rock deposition to up to ~10 My later; and they are hosted by carbonates within a  
1032 carbonate-shale sequence. The deposits were probably produced by convective flow systems that  
1033 developed many of the geological features more commonly associated with Sedex than with MVT  
1034 deposits, including higher fluid temperatures and lower salinities, footwall (classic epigenetic) feeder  
1035 vein and breccia zones, and strong zoning on the deposit scale in terms of metals and alteration  
1036 patterns (e.g., Ashton et al., 1992; Fusciardi et al., 2003; Lowther et al., 2003). The recognition of  
1037 significant heterogeneity in fluid chemistry in Ireland (and in the metal tenor of resulting deposits)  
1038 may reflect an intrinsic character of convective flow systems that might be anticipated in other Sedex  
1039 provinces.

1040 The derivation of a range of components from the underlying low-grade metamorphic basement  
1041 can be convincingly demonstrated (Pb, Sr) or inferred (Li, Ca, Ba, Mn, Fe, Co, Ni, Cu, Zn, As). Fluids  
1042 flowing within extensive fracture permeability in this metal-fertile, arc-derived greywacke-shale  
1043 ( $\pm$ volcanic) succession are clearly capable of efficiently extracting metals. This implies that basement

1044 involvement could be important in other sediment-hosted systems, and the common assumption  
1045 that fluids and metals are solely derived from basinal clastic successions (e.g., Goodfellow et al.,  
1046 1993; Leach et al., 2005) should be tested critically. The potential for surficial recharge of fluids, as  
1047 documented in Ireland, means that the system is not intrinsically fluid volume-limited enabling  
1048 potentially greater metal mobilization. Such deep crustal circulation is probably a requirement in  
1049 basin environments where subsidence has been limited and basin successions are consequently thin;  
1050 however, it may not be required in long-lived intracratonic basins (typified by many Proterozoic  
1051 systems), where basin sequences may be in excess of 10 km.

1052 A complex evolution in pore fluid chemistry in the carbonate host rocks can be documented from  
1053 early, seawater-related diagenetic fluids (based mainly on textures and marine carbon and oxygen  
1054 isotope signatures) that were replaced by progressively hotter hydrothermal fluids (from textures  
1055 and fluid inclusion, carbon, oxygen and strontium isotope data). Later brines then dolomitized  
1056 younger sediments and overprinted the ore deposits. All these fluids were derived ultimately from  
1057 seawater, and the ambient paleoclimate and paleotopography played a key role in controlling fluid  
1058 heterogeneity and possibly fluid fertility, as well as recharge. The evolution of brine chemistry and  
1059 the flow pathways utilized are likely to be a function of the detailed paleogeography/  
1060 geomorphology, distribution and diagenesis of sedimentary facies, and basin floor/margin  
1061 permeability as is highlighted in studies of modern intracratonic basins (e.g. Stanislavsky and  
1062 Gvirtzman, 1999; Stein et al., 2000; Klein-BenDavid et al., 2004). Consequently, significant complexity  
1063 should be expected in fluid origins in intracratonic basin-hosted ore districts elsewhere, but these  
1064 can be resolved with careful application of modern microchemical analyses of fluid inclusions.

1065

#### 1066 *Concluding remarks*

1067 The Irish orefield presents arguably the best database available on the thermal and chemical  
1068 characteristics of hydrothermal fluids involved in sediment-hosted ore genesis and is an excellent  
1069 example of a fossil, crustal scale hydrothermal system. As such, it provides a valuable laboratory that  
1070 could be used for further understanding the dynamics of flow, the chemical exchange and the origin,  
1071 transport and deposition of metals during seawater-crust interaction. Outcrop access to various parts  
1072 of the stratigraphic record in Ireland, coupled with mine exposures and extensive drillcore has  
1073 allowed a three dimensional understanding of the hydrothermal system to be developed. Fluid  
1074 inclusion measurements, together with careful paragenetic studies that require the use of detailed  
1075 textural analytical tools such as cathodoluminescence, have allowed the system to be examined as a  
1076 function of relative time. Future geochronology is desirable, although the interpretation of  
1077 increasingly precise geochronological ages will remain problematic in the absence of finely resolved  
1078 stratigraphic dating in the Lower Carboniferous. Regional-scale sampling has identified large-scale

1079 heterogeneity in fluid properties and the data indicate complex fluid-fluid and fluid-rock interaction  
1080 processes at the local scale. Although a start has been made, further work comparing and  
1081 interpreting thermal, chemical and isotopic tracers in the ore systems with those in weakly  
1082 mineralized prospects is needed to better understand the processes controlling the localization of  
1083 economic mineralization.

1084

#### 1085 **Acknowledgments**

1086 The data presented in this paper is a compilation of results from the author and several PhD  
1087 students who have worked on the Irish system over the past decade: Sally Eyre, the late Kate Everett,  
1088 Mike Lee and Helen Crowther. Their work has been critical to the development of the ideas  
1089 presented. I would also like to thank the many others who have facilitated, encouraged and inspired  
1090 my Irish endeavours. In particular in Ireland: John Ashton, Rob Blakeman, Dave Blaney, Mike Boland,  
1091 Andy Bowden, Eibhlihn Doyle, Garth Earls, Leo Fusciardi, Steve Gatley, Jim Geraghty, Jay Gregg, John  
1092 Güven, Mark Holdstock, Murray Hitzman, the late Dave Johnston, John Kelly, Mike Lowther, Paul  
1093 McDermott, George Sevastopulo, Ed Slowey, Gerry Stanley; and at SUERC, East Kilbride, Adrian  
1094 Boyce, Tony Fallick, and support staff. The inspiration and creative thinking of Mike Russell have  
1095 always been a challenge and a motivation. Many discussions with these and others have informed  
1096 my understanding of the geology of Ireland, but any errors or omissions in this paper are my own.  
1097 The careful and constructive reviews of Iain Samson and an anonymous referee helped to improve  
1098 the paper significantly. Research has been supported by Natural Environment Research Council  
1099 grants GR9/03047, **Micro-to-macro project**, IP/528/0997, the University of London Central Research  
1100 Fund, SEG Hugh McKinstry grants, Anglo Base Metals Ireland, Arcon Mines, BHP Minerals, CSA Ltd,  
1101 Glencar plc, Lundin Mining, New Boliden, and Outokumpu Zinc.



1102 **References**

1103

1104 Agrinier, P., Hékinian, R., Bideau, D., and Javoy, M., 1995, O and H stable isotope compositions of  
1105 oceanic crust and upper mantle rocks exposed in the Hess Deep near the Galapagos Triple Junction:  
1106 Earth and Planetary Science Letters, v. 136, p. 183-196.

1107

1108 Allan, J.R., Beaty, D.W., Sturtevant, R.G., Hitzman, M.W., and Shearley, E., 1992, The origin of  
1109 regional dolomite in the Waulsortian of southeastern Ireland: implications for ore deposition [abs]:  
1110 Geological Society of America, Abstracts with Programs, v. 24, p. A354.

1111

1112 Anderson, I.K., Ashton, J.H., Earls, G., Hitzman, M.W., and Tear, S., eds., 1995, Irish Carbonate-hosted  
1113 Zn-Pb Deposits. Society of Economic Geologists Guidebook Series, Volume 21.

1114

1115 Anderson, I.K., Ashton, J.H., Boyce, A.J., Fallick, A.E., and Russell, M.J., 1998, Ore depositional  
1116 processes in the Navan Zn + Pb deposit, Ireland: ECONOMIC GEOLOGY, v. 93, p. 535-563.

1117

1118 Andrew, C.J., 1993, Mineralization in the Irish Midlands, in Patrick, R.A.D. and Polya, D.A., eds.,  
1119 Mineralization in the British Isles: London, Chapman and Hall, p. 208-269.

1120

1121 Andrew, C.J., Crowe, R.W.A., Finlay, S., Pennell, W.M., and Pyne, J., eds., 1986, Geology and genesis  
1122 of mineral deposits in Ireland: Dublin, Irish Association for Economic Geology, 711 pp.

1123

1124 Ashton, J.H., Downing, D.T., and Finlay, S., 1986, The geology of the Navan Zn-Pb orebody, in Andrew,  
1125 C.J., Crowe, R.W.A., Finlay, S., Pennell, W.M. and Pyne, J., eds., Geology and genesis of mineral  
1126 deposits in Ireland: Dublin, Irish Association for Economic Geology, p. 243-280.

1127

1128 Ashton, J.H., Black, A., Geraghty, J., Holdstock, M., and Hyland, E., 1992, The geological setting and  
1129 metal distribution patterns of Zn-Pb-Fe mineralization in the Navan Boulder Conglomerate, in  
1130 Bowden, A.A., Earls, G., O'Connor, P.G., and Pyne, J.F., eds., The Irish Minerals Industry 1980-1990:  
1131 Dublin, Irish Association for Economic Geology, p. 171-197.

1132

1133 Banks, D.A., 1985, A fossil hydrothermal worm assemblage from the Tynagh lead-zinc deposit in  
1134 Ireland: Nature, v. 313, p. 128-131.

1135

1136 Banks, D.A., and Russell, M.J., 1992, Fluid mixing during ore deposition at the Tynagh base metal  
1137 deposit, Ireland: *European Journal of Mineralogy*, v. 4, p. 921-931.  
1138

1139 Banks, D.A., Boyce, A.J., and Samson, I.M., 2002, Constraints on the Origins of fluids forming Irish Zn-  
1140 Pb-Ba deposits: Evidence from the composition of fluid Inclusions: *ECONOMIC GEOLOGY*, v. 97, p.  
1141 471-480.  
1142

1143 Blakeman, R., Ashton, J.H., Boyce, A.J., Fallick, A.E., and Russell, M.J., 2002, Timing of interplay  
1144 between hydrothermal and surface fluids in the Navan Zn+Pb orebody, Ireland: Evidence from metal  
1145 distribution trends, mineral textures and  $\delta^{34}\text{S}$  analyses: *ECONOMIC GEOLOGY*, v. 97, p. 73-91.  
1146

1147 Boast, A.M., Coleman, M.L., and Halls, C., 1981, Textural and stable isotopic evidence for the genesis  
1148 of the Tynagh base metal deposit, Ireland: *ECONOMIC GEOLOGY*, v. 76, p. 27-55.  
1149

1150 Bodnar, R.J., 2003a, Re-equilibration of fluid inclusions, in Samson, I., Anderson, A., and Marshall, D.,  
1151 eds., *Fluid Inclusions: Analysis and Interpretation: Mineralogical Association of Canada Short Course*  
1152 *32*, Chapter 4.  
1153

1154 Bodnar, R.J., 2003b, Interpretation of data from aqueous-electrolyte fluid inclusions, in Samson, I.,  
1155 Anderson, A., and Marshall, D., eds., *Fluid Inclusions: Analysis and Interpretation: Mineralogical*  
1156 *Association of Canada Short Course 32*, Chapter 8.  
1157

1158 Bodnar, R.J., and Bethke, P.M., 1984, Systematics of stretching of fluid inclusions I: Fluorite and  
1159 sphalerite at 1 atmosphere confining pressure: *ECONOMIC GEOLOGY*, v. 79, p. 141-161.  
1160

1161 Bodnar, R.J., Binns, P.R., and Hall, D.L., 1989, Synthetic fluid inclusions – VI. Quantitative evaluation  
1162 of the decrepitation behaviour of fluid inclusions in quartz at one atmosphere confining pressure:  
1163 *Journal of Metamorphic Geology*, v. 7, p. 229-242.  
1164

1165 Bowden, A.A., Earls, G., O'Connor, P.G., and Pyne, J.F., eds., 1992, *The Irish Minerals Industry 1980-*  
1166 *1990: Dublin, Irish Association for Economic Geology*, 434 p.  
1167

1168 Boyce, A.J., Anderton, R., and Russell, M.J., 1983, Rapid subsidence and early Carboniferous  
1169 mineralisation in Ireland: *Transactions of the Institution of Mining and Metallurgy*, v. 92, p. B55-66.  
1170

1171 Boyce, A.J., Little, C.T.S., and Russell, M.J., 2003, A new fossil vent biota in the Ballynoe barite  
1172 deposit, Silvermines, Ireland: Evidence for intracratonic sea-floor hydrothermal activity about 352  
1173 Ma: ECONOMIC GEOLOGY, v. 98, p. 649-656.  
1174

1175 Burruss, R.C., 1987, Diagenetic palaeotemperatures from aqueous fluid inclusions: re-equilibration of  
1176 inclusions in carbonate cements by burial heating: Mineralogical Magazine, v. 51, p. 477-481.  
1177

1178 Caulfield, J.B.D., LeHuray, A.P., and Rye, D.M., 1986, A review of lead and sulphur isotope  
1179 investigations of Irish sediment-hosted base metal deposits, with new data from Keel, Ballinalack,  
1180 Moyvoughly and Tatestown deposits, in Andrew, C.J., Crowe, R.W.A., Finlay, S., Pennell, W.M., and  
1181 Pyne, J., eds., Geology and genesis of mineral deposits in Ireland: Dublin, Irish Association for  
1182 Economic Geology, p. 591-616.  
1183

1184 Clayton, G., Haughey, N., Sevastopulo, G.D., and Burnett, R., 1989, Thermal maturation levels in the  
1185 Devonian and Carboniferous rocks in Ireland. Dublin, Geological Survey of Ireland, 36 p.  
1186

1187 Corbett, G., 2004, Epithermal and porphyry gold – Geological models, in Proceedings of the PACRIM  
1188 2004 Congress, Adelaide: Melbourne, Australian Institute of Mining and metallurgy, p. 15-23.  
1189

1190 Crowther, H.L., 2007, A rare earth element and transition metal isotope study of the Irish Zn-Pb  
1191 orefield: Unpub. Ph.D. thesis, University of London, 198 p.  
1192

1193 Dix, G.R., and Edwards, C., 1996, Carbonate-hosted, shallow-submarine and burial hydrothermal  
1194 mineralization in the Upper Mississippian Big Cove Formation, Port au Port Peninsula,  
1195 Western Newfoundland: ECONOMIC GEOLOGY, v. 91, p. 180-203.  
1196

1197 Dixon, P.R., 1990, The role of basement-circulated fluids in the origin of sediment-hosted Zn-Pb-Ba  
1198 mineralization in Ireland: Unpub. Ph.D. thesis, Yale University, 249 p.  
1199

1200 Doyle, E., Bowden, A.A., Jones, G.V., and Stanley, G.A., 1992, The geology of the Galmoy deposits, in  
1201 Bowden, A.A., Earls, G., O'Connor, P.G., and Pyne, J.F., eds., The Irish Minerals Industry 1980-1990:  
1202 Dublin, Irish Association for Economic Geology, p. 211-225.  
1203

1204 Emo, G.T., 1986, Some considerations regarding the styles of mineralization at Harberton Bridge, Co.  
1205 Kildare, in Andrew, C. J., Crowe, R. W. A., Finlay, S., Pennell, W. M. and Pyne, J., eds., *Geology and*  
1206 *genesis of mineral deposits in Ireland*: Dublin, Irish Association for Economic Geology, p. 461-470.  
1207

1208 Everett, C.E., 1999, *Tracing ancient fluid flow pathways: A study of the Lower Carboniferous base*  
1209 *metal orefield in Ireland*: Unpub. Ph.D. thesis, Yale Univ., 354 p.  
1210

1211 Everett C.E., Wilkinson, J.J., and Rye, D.M., 1999a, *Fracture-controlled fluid flow in the Lower*  
1212 *Palaeozoic basement rocks of Ireland: Implications for the genesis of Irish-type Zn-Pb deposits*, in  
1213 McCaffrey, K.J.W., Lonergan, L. and Wilkinson, J.J., eds., *Fractures, Fluid Flow and Mineralization*:  
1214 *Geological Society of London, Special Publications*, v. 155, p. 247-276.  
1215

1216 Everett, C.E., Wilkinson, J.J., Boyce, A.J., Ellam R., Gleeson, S.A., Rye, D.M., and Fallick, A.E., 1999b,  
1217 *The genesis of Irish-type base metal deposits: Characteristics and origins of the principal ore fluid*, in  
1218 Stanley, C.J. et al., eds., *Mineral Deposits; Processes to Processing*: Rotterdam, A.A. Balkema, p. 845-  
1219 848.  
1220

1221 Everett, C.E., Rye, D.M., and Ellam, R.M., 2003, *Source or sink? An assessment of the role of the Old*  
1222 *Red Sandstone in the genesis of the Irish Zn-Pb deposits*: *ECONOMIC GEOLOGY*, v. 98, p. 31-50.  
1223

1224 Eyre, S.L., 1998, *Geochemistry of dolomitization and Zn-Pb mineralization in the Rathdowney Trend,*  
1225 *Ireland*: Unpub. Ph.D. thesis, Univ. London, 414 p.  
1226

1227 Eyre, S.L., Wilkinson, J.J., Stanley, C.J., Boyce, A.J., 1996, *Geochemistry of dolomitisation and zinc-*  
1228 *lead mineralisation in the Rathdowney Trend, Ireland [abs]*: *Geological Society of America, Abstracts*  
1229 *with Programs*, v. 28, p. A210-211.  
1230

1231 Fournier, R.H., and Truesdell, A.H., 1973, *An empirical Na-K-Ca geothermometer for natural waters.*  
1232 *Geochimica et Cosmochimica Acta*, v. 37, p. 1255-1275.  
1233

1234 Fusciardi, L.P., Guven, J.F., Stewart, D.R.A., Carboni, V., and Walshe, J.J., 2003, *The geology and*  
1235 *genesis of the Lisheen Zn-Pb deposit, Co. Tipperary, Ireland*, in Kelly, J.G., Andrew, C.J., Ashton, J.H.,  
1236 Boland, M.B., Earls, G., Fusciardi, L., and Stanley, G., eds., *Europe's Major Base Metal Deposits*:  
1237 *Dublin, Irish Association for Economic Geology*, p. 455-481.  
1238

1239 Giggenschbach, W.F., 1988, Geothermal solute equilibria. Derivation of Na-K-Mg-Ca geothermometers.  
1240 *Geochimica et Cosmochimica Acta*, v. 52, p. 2749-2765.  
1241  
1242 Gleeson, S.A., Banks, D.A., Everett, C.E., Wilkinson, J.J., Samson, I.M., and Boyce, A.J., 1999, Origin of  
1243 mineralising fluids in Irish-type deposits: constraints from halogen analyses, in Stanley, C.J. et al.,  
1244 eds., *Mineral Deposits; Processes to Processing*: Rotterdam, A.A. Balkema, p. 857-860.  
1245  
1246 Gleeson, S.A., Wilkinson, J.J., Stuart, F.M., and Banks, D.A., 2001, The origin and chemical evolution  
1247 of base metal mineralising formation waters and hydrothermal fluids, South Cornwall, U.K.:  
1248 *Geochimica et Cosmochimica Acta*, v. 65, p. 2067-2079.  
1249  
1250 Goodfellow, W.D., Lydon, J.W., and Turner, R.W., 1993, Geology and genesis of stratiform sediment-  
1251 hosted (SEDEX) Zn-Pb-Ag sulphide deposits: Geological Association of Canada, Special Paper 40, p.  
1252 201-251.  
1253  
1254 Goodhue, R., and Clayton, G., 1999, Organic maturation levels, thermal history and hydrocarbon  
1255 source rock potential of the Namurian rocks of the Clare Basin, Ireland: *Marine and Petroleum*  
1256 *Geology*, v. 16, p. 667-675.  
1257  
1258 Gregg, J.M., Shelton, K.L., Johnson, A.W., Somerville, I.D., and Wright, W.R., 2001, Dolomitization of  
1259 the Waulsortian Limestone (Lower Carboniferous) in the Irish Midlands: *Sedimentology*, v. 48, p. 745-  
1260 766.  
1261  
1262 Greig, J.A., Baadsgard, H., Cumming, G.L., Folinsbee, R.E., Krouse, H.R., Ohmoto, H., Sasaki, A. and  
1263 Smejkal, V., 1971, Lead and sulfur isotopes of the Irish base metal mines in Carboniferous carbonate  
1264 host rocks: Proceedings of the joint IMA-IAGOD meeting, Tokyo, 1970. Society of Mining Geologists  
1265 of Japan, Special Issue No. 2, p. 84-92.  
1266  
1267 Grennan, E.F., 1986, Geology and genesis of the Courtbrown Pb-Zn-Ag deposit, in Andrew, C.J.,  
1268 Crowe, R.W.A., Finlay, S., Pennell, W.M. and Pyne, J., eds., *Geology and genesis of mineral deposits in*  
1269 *Ireland*: Dublin, Irish Association for Economic Geology, p. 449-455.  
1270  
1271 Hitzman, M.W., 1986, Geology of the Abbeytown Mine, Co. Sligo, Ireland, in Andrew C.J., Crowe,  
1272 R.W.A., Finlay, S., Pennell, W.M., and Pyne, J., eds., *Geology and genesis of mineral deposits in*  
1273 *Ireland*: Dublin, Irish Association for Economic Geology, p. 341-353.

1274

1275 Hitzman, M.W., 1995, Geological setting of the Irish Zn-Pb-(Ba-Ag) orefield, in Anderson, I.K., Ashton,  
1276 J.H., Earls, G., Hitzman, M.W., and Tear, S., eds., Irish Carbonate-hosted Zn-Pb Deposits: Society of  
1277 Economic Geologists Guidebook Series, v. 21, p. 3-23.

1278

1279 Hitzman, M.W. and Beaty, D.W., 1996, The Irish Zn-Pb-(Ba) orefield, in Sangster, D.F., ed., Carbonate-  
1280 hosted lead-zinc deposits: Society of Economic Geologists, Special Publication, v. 4, p. 112-143.

1281

1282 Hitzman, M.W., and Large, D.E., 1986, A review and classification of the Irish carbonate-hosted base  
1283 metal deposits, in Andrew, C.J., Crowe, R.W.A., Finlay, S., Pennell, W.M., and Pyne, J., eds., Geology  
1284 and genesis of mineral deposits in Ireland: Dublin, Irish Association for Economic Geology, p. 217-  
1285 238.

1286

1287 Hitzman, M.W., O'Connor, P.G., Shearley, E., Schaffalitzky, C., Beatty, D.W., Allan, J.R., and  
1288 Thompson, T., 1992, Discovery and geology of the Lisheen Zn-Pb-Ag prospect, Rathdowney Trend,  
1289 Ireland, in Bowden, A.A., Earls, G., O'Connor, P.G., and Pyne, J.F., eds., The Irish Minerals Industry  
1290 1980-1990: Dublin, Irish Association for Economic Geology, p. 227-246.

1291

1292 Hitzman, M.W., Earls, G., Shearley, E., Kelly, J., Cruise, M., and Sevastopulo, G., 1995, Ironstones (iron  
1293 oxide-silica) in the Irish Zn-Pb deposits and regional iron oxide-(silica) alteration of the Waulsortian  
1294 limestone in southern Ireland, in Anderson, I.K., Ashton, J.H., Earls, G., Hitzman, M.W., and Tear, S.,  
1295 eds., Irish Carbonate-hosted Zn-Pb Deposits: Society of Economic Geologists Guidebook Series, v. 21,  
1296 p. 261-273.

1297

1298 Hitzman, M.W., Allan, J.R., and Beaty, D.W., 1998, Regional dolomitization of the Waulsortian  
1299 limestone in southeastern Ireland: evidence of large-scale fluid flow driven by the Hercynian  
1300 orogeny: *Geology*, v. 26, p. 547-550.

1301

1302 Hitzman, M.W., Redmond, P.B., and Beaty, D.W., 2002, The carbonate-hosted Lisheen Zn-Pb-Ag  
1303 deposit, County Tipperary, Ireland: *ECONOMIC GEOLOGY*, v. 97, p. 1627-1655.

1304

1305 Holdstock, M.P., 1982, Breccia hosted zinc-lead mineralization in Tournasian and Lower Viséan  
1306 carbonates at Harberton Bridge, Co. Kildare, in Brown, A.G., ed., *Mineral Exploration in Ireland,*  
1307 *Progress and Developments 1971-1981:* Dublin, Irish Association for Economic Geology, p. 83-91.

1308

1309 Holdstock, M.P., 1983, The Lower Carboniferous geology and base metal mineralization of northeast  
1310 County Kildare, Ireland. Unpub. Ph.D. thesis, National University of Ireland.  
1311

1312 Johnson, A.W., Shelton, K.L., Gregg, J.M., Somerville, I.D., and Wright, W.R., 2001, Fluid inclusion  
1313 evidence for the presence of multiple fluids in Zn-Pb hosting carbonate rocks in the Irish Midlands:  
1314 Initial findings, in Hagni, R.D., ed., Studies on ore deposits, mineral economics and applied  
1315 mineralogy: University of Missouri-Rolla, p. 18-30.  
1316

1317 Johnson, A.W., Shelton, K.L., Gregg, J.M., Somerville, I.D., Wright, W.R., and Nagy, Z.R., 2009,  
1318 Regional studies of dolomites and their included fluids: recognizing multiple chemically distinct fluids  
1319 during the complex diagenetic history of Lower Carboniferous (Mississippian) rocks of the Irish Zn-Pb  
1320 ore field: Mineralogy and Petrology, DOI 10.1007/s00710-008-0038-x.  
1321

1322 Jones, G.L., 1992, Irish Carboniferous conodonts record maturation levels and the influence of  
1323 tectonism, igneous activity and mineralization: Terra Nova, v. 4, p. 228-234.  
1324

1325 Kelly, J.G., Andrew, C.J., Ashton, J.H., Boland, M.B., Earls, G., Fusciardi, L., and Stanley, G., eds., 2003,  
1326 Europe's Major Base Metal Deposits: Dublin, Irish Association for Economic Geology, 552 p.  
1327

1328 Kennan, P.S., Phillips, W.E.A. and Strogon, P., 1979, Pre-Caledonian basement to the paratectonic  
1329 Caledonides in Ireland: Geological Society of London, Special Publications, v. 8, p. 157-161.  
1330

1331 Klein-BenDavid, O., Sass, E., and Katz, A., 2004, The evolution of marine evaporitic brines in inland  
1332 basins: The Jordan–Dead Sea Rift valley: Geochimica et Cosmochimica Acta, v. 68, p. 1763-1775.  
1333

1334 Knauth, L.P., and Beeunas, M.A., 1985, Isotope geochemistry of fluid inclusions in Permian halite with  
1335 implications for the isotopic history of ocean water and the origin of saline formation waters:  
1336 Geochimica et Cosmochimica Acta, v. 50, p. 419-433.  
1337

1338 Leach, D.L., Sangster, D.L., Kelley, K.D., Large, R.R., Garven, G., Allen, C.R., Gutzmer, J., and Walter, S.,  
1339 2005, Sediment-hosted lead-zinc deposits: A global perspective: Society of Economic Geologists, One  
1340 Hundredth Anniversary Volume 1905-2005, p. 561-607.  
1341

1342 Lee, M.J., 2002, Origin and Zn-Pb mineralization of dolomite breccias in the Irish Midlands: Unpub.  
1343 Ph.D. thesis, Univ. London, 256 p.

1344

1345 Lee, M.J., and Wilkinson, J.J., 2002, Cementation, hydrothermal alteration, and Zn-Pb mineralization  
1346 of carbonate breccias in the Irish Midlands: Textural evidence from the Cooleen Zone, near  
1347 Silvermines, County Tipperary: *ECONOMIC GEOLOGY*, v. 97, p. 653-662.

1348

1349 Lees, A., and Miller, J., 1995, Waulsortian banks, in Monty, C.L.V., Bosence, D.W.J., Bridges, P.H., and  
1350 Pratt, B.R., eds., *Carbonate Mud-Mounds*: Oxford, Blackwell Science, International Association of  
1351 Sedimentologists Special Publication 23, p. 191-271.

1352

1353 Lepp, H., 1957, The synthesis and probable geologic significance of melnikovite: *ECONOMIC*  
1354 *GEOLOGY*, v. 52, p. 528-535.

1355 Lowenstein, T.K., Hardie, L.A., Timofeeff, M.N., and Demicco, R.V., 2003, Secular variation in  
1356 seawater chemistry and the origin of calcium chloride basinal brines: *Geology*, v. 31, p. 857-860.

1357

1358 Lowther, J.M., Balding, A.B., McEvoy, F.M., Dunphy, S., MacEoin, P., Bowden, A.A., and McDermott,  
1359 P., 2003, The Galmoy Zn-Pb orebodies: structure and metal distribution – clues to the genesis of the  
1360 deposits, in Kelly, J.G., Andrew, C.J., Ashton, J.H., Boland, M.B., Earls, G., Fuscuardi, L., and Stanley, G.,  
1361 eds., *Europe's Major Base Metal Deposits*: Dublin, Irish Association for Economic Geology, p. 437-  
1362 454.

1363

1364 Lydon, J. W., 1986, A model for the generation of metalliferous hydrothermal solutions in a  
1365 sedimentary basin, and its application to the Irish Carboniferous base metal deposits, in Andrew, C.  
1366 J., Crowe, R. W. A., Finlay, S., Pennell, W. M. and Pyne, J., eds., *Geology and genesis of mineral*  
1367 *deposits in Ireland*: Dublin, Irish Association for Economic Geology, p. 555-577.

1368

1369 McCaffrey, M.A., Lazar, B., and Holland, H.D., 1987, The evaporation path of seawater and the  
1370 coprecipitation of  $\text{Br}^-$  and  $\text{K}^+$  with halite: *Journal of Sedimentary Petrology*, v. 57, p. 928-937.

1371

1372 Mulhall, C.M., 2003, An investigation of the fluids involved in the formation of some Irish Lower  
1373 Carboniferous dolomites: Unpub. Ph.D. thesis, Trinity College Dublin, 325 p.

1374

1375 Naden, J., 1996. CalcicBrine 1.5: a Microsoft Excel 5.0 add-in for calculating salinities from  
1376 microthermometric data in the system  $\text{NaCl-CaCl}_2\text{-H}_2\text{O}$  [abs]: PACROFI VI, Abstracts Volume,  
1377 University of Wisconsin, Madison, USA, p. 97-98.

1378



1379 Nagy, Z.R., Gregg, J.M., Becker, S.P., Somerville, I.D., Shelton, K.L., and Johnson, A.W., 2004, Early  
1380 dolomitisation and fluid migration through the Lower Carboniferous carbonate platform in the  
1381 southeast Irish Midlands: Implications for reservoir attributes, in Braithwaite C.J.R., Rizzi G., and  
1382 Darke G., eds., *The Geometry and Petrogenesis of Dolomite Hydrocarbon Reservoirs: Geological*  
1383 *Society of London, Special Publications*, v. 235, p. 367-392.

1384

1385 Nunn, J.A., 1994, Free thermal convection beneath intracratonic basins: thermal and subsidence  
1386 effects: *Basin Research*, v. 6, p. 115-130.

1387

1388 O'Reilly, C., Fallick, A.E., Jenkin, G.R.T., Feely, M., and Alderton, D.H.M., 1997a, fluid inclusion and  
1389 stable isotope study of 200 Ma of fluid evolution in the Galway Granite, Connemara, Ireland:  
1390 *Contributions to Mineralogy and Petrology*, v. 585, p. 120-142.

1391

1392 O'Reilly, C., Feely, M., Holdstock, M.P., and O'Keefe, W.G., 1997b, Fluid inclusion study of the  
1393 unexposed Kentstown Granite, Co. Meath, Ireland: *Transactions of the Institution of Mining and*  
1394 *Metallurgy*, v. 107, B31-37.

1395

1396 Patterson, J.M., 1970, *Geology and mineralisation of the Keel area, Co. Longford, Ireland: Unpub.*  
1397 *Ph.D. thesis, Univ. London*, 274 p.

1398

1399 Peace, W.M., 1999, *Carbonate-hosted Zn-Pb mineralisation within the Upper Pale Beds at Navan,*  
1400 *Ireland: Unpub. Ph.D. thesis, Univ. Melbourne*, 284 p.

1401

1402 Peace, W.M., Wallace, M.W., Holdstock, M.P., and Ashton, J.H., 2003, Ore textures within the U lens  
1403 of the Navan Zn-Pb deposit, Ireland: *Mineralium Deposita*, v. 38, p. 568–584.

1404

1405 Philcox, M.E., 1984, *Lower Carboniferous lithostratigraphy of the Irish Midlands: Dublin, Irish*  
1406 *Association for Economic Geology*, 89 p.

1407

1408 Phillips, W.E.A., and Sevastopulo, G.D., 1986, The stratigraphic and structural setting of Irish mineral  
1409 deposits, in Andrew, C.J., Crowe, R.W.A., Finlay, S., Pennell, W.M., and Pyne, J., eds., *Geology and*  
1410 *genesis of mineral deposits in Ireland: Dublin, Irish Association for Economic Geology*, p. 1-30.

1411

1412 Probert, K., 1983, Fluid inclusion data from carbonate hosted Irish base metal deposits [abs]: Mineral  
1413 Deposits Studies Group Annual Meeting, Programme with Abstracts, University of Manchester,  
1414 Manchester, UK.  
1415

1416 Reed, C.P., and Wallace, M.W., 2001, Diagenetic evidence for an epigenetic origin of the Courtbrown  
1417 Zn-Pb deposit, Ireland: *Mineralium Deposita*, v. 36, p. 428-441.  
1418

1419 Rejebian, V.A., Harris, A.G., and Huebner, J.S., 1987, Conodont color and textural alteration; an index  
1420 to regional metamorphism, contact metamorphism, and hydrothermal alteration: *Geological Society  
1421 of America Bulletin*, v. 99, p. 471-479.  
1422

1423 Rizzi, G., and Braithwaite, C.J.R., 1997, Sedimentary cycles and selective dolomitization in limestones  
1424 hosting the giant Navan zinc-lead ore deposit, Ireland: *Exploration and Mining Geology*, v. 6, p. 63-77.  
1425

1426 Roedder, E., 1976, Fluid inclusion evidence on the genesis of ores in sedimentary and volcanic rocks,  
1427 in Wolf, K.H., ed., *Handbook of Strata-bound and Stratiform Ore Deposits; I. Principles and General  
1428 Studies; Vol. 2, Geochemical studies*: New York, Elsevier, p. 67-110.  
1429

1430 Roedder, E., 1984, Fluid Inclusions: *Mineralogical Society of America, Reviews in Mineralogy*, v. 12,  
1431 644 p.  
1432

1433 Russell, M.J., 1978, Downward-excavating hydrothermal cells and Irish type ore deposits: importance  
1434 of an underlying thick Caledonian prism: *Transactions of the Institution of Mining and Metallurgy*, v.  
1435 87, p. B168-171.  
1436

1437 Russell, M.J., 1986, Extension and convection: a genetic model for the Irish Carboniferous base metal  
1438 and barite deposits, in Andrew, C.J., Crowe, R.W.A., Finlay, S., Pennell, W.M. and Pyne, J., eds.,  
1439 *Geology and genesis of mineral deposits in Ireland*: Dublin, Irish Association for Economic Geology, p.  
1440 545-554.  
1441

1442 Russell, M.J., Solomon, M., and Walshe, J.L., 1981, The genesis of sediment-hosted exhalative zinc +  
1443 lead deposits: *Mineralium Deposita*, v. 16, p. 113-127.  
1444

1445 Samson, I.M., 1983, Fluid inclusion and stable isotope studies of the Silvermines orebodies, Ireland,  
1446 and comparisons with Scottish vein deposits: Unpub. Ph.D. thesis, Glasgow, Univ. Strathclyde, 290 p.

1447  
1448 Samson, I.M. and Russell, M.J., 1983, Fluid inclusion data from Silvermines base metal – barite  
1449 deposits, Ireland: Transactions of the Institution of Mining and Metallurgy, v. 92, B67-71.  
1450  
1451 Samson, I.M. and Russell, M.J., 1987, Genesis of the Silvermines zinc-lead-barite deposit, Ireland:  
1452 Fluid inclusion and stable isotope evidence: ECONOMIC GEOLOGY, v. 82, p. 371-394.  
1453  
1454 Sangster, D.F., 1990, Mississippi Valley-type and SEDEX lead-zinc deposits: A comparative  
1455 examination: Transactions of the Institution of Mining and Metallurgy, v. 99, p. B21-42.  
1456  
1457 Slowey, E.P., 1986, The zinc-lead and barite deposits at Keel, Co. Longford, in Andrew, C.J., Crowe,  
1458 R.W.A., Finlay, S., Pennell, W.M., and Pyne, J., eds., 1986, Geology and Genesis of Mineral Deposits in  
1459 Ireland: Dublin, Irish Association for Economic Geology, p. 319-330.  
1460  
1461 Slowey, E.P., Hitzman, M.W., Beaty, D.W., and Thompson, T.B., 1995, The Keel Zn-Pb and Garrycam  
1462 BaSO<sub>4</sub> deposits, Co. Longford, Ireland, in Anderson, I.K., Ashton, J.H., Earls, G., Hitzman, M.W., and  
1463 Tear, S., eds., Irish Carbonate-hosted Zn-Pb Deposits, Guidebook Series, v. 21: Society of Economic  
1464 Geologists, p. 227-241.  
1465  
1466 Stanislavsky, E. and Girtzman, H., 1999, Basin-scale migration of continental-rift brines:  
1467 Paleohydrologic modeling of the Dead Sea basin: Geology, v. 27, p. 791-794.  
1468  
1469 Stein, M., Starinsky, A., Agnon, A., Katz, A., Raab, M., Spiro, B., and Zak, I., 2000, The impact of brine-  
1470 rock interaction during marine evaporite formation on the isotopic Sr record in the oceans: Evidence  
1471 from Mt. Sedom, Israel: Geochimica et Cosmochimica Acta, v. 64, p. 2039-2053.  
1472  
1473 Stoffell, B., Wilkinson, J.J., and Jeffries, T.E., 2004, Metal transport and deposition in hydrothermal  
1474 veins revealed by 213nm UV laser ablation microanalysis of single fluid inclusions: American Journal  
1475 of Science, v. 304, p. 533-557.  
1476  
1477 Strogon, P., 1974, The sub-Palaeozoic basement in central Ireland: Nature, v. 250, p. 562-563.  
1478  
1479 Taylor, S., 1984, Structural and paleotopographical controls of lead-zinc mineralization in the  
1480 Silvermines ore bodies, Republic of Ireland: ECONOMIC GEOLOGY, v. 79, p. 529-548.  
1481

1482 Thomas, L.J., Harmon, R.S., and Oliver, G.J.H., 1985, Stable isotope composition of alteration fluids in  
1483 low-grade Lower Palaeozoic rocks, English Lake District: *Mineralogical Magazine*, v. 49, p. 425-434.  
1484

1485 Thompson, T.B., 1992, Mineralogy and fluid inclusion analyses of the Garrycam/Keel Zn-Ba-Pb-Ag  
1486 system, County Longford, Ireland: Unpublished report for Chevron Oil Field Research Company, 9 p.  
1487

1488 Thompson, T.B., Hitzman, M.W., and Beaty, D.W., 1992, Paragenesis and fluid inclusions of the  
1489 Lisheen Zn-Pb-Ag deposit, Co. Tipperary, Ireland [abs]: *Geological Society of America, Abstracts with*  
1490 *Programs*, v. 24, p. A354.  
1491

1492 Trude, K.J., and Wilkinson, J.J., 2001, A mineralogical and fluid inclusion study of the Harberton  
1493 Bridge Fe-Zn-Pb deposit, County Kildare, Ireland: *Journal of the Geological Society, London*, v. 158, p.  
1494 37-46.  
1495

1496 Ulrich, M.R., and Bodnar, R.J., 1988, Systematics of stretching of fluid inclusions II: Barite at 1 Atm  
1497 confining pressure: *Economic Geology*, v. 83, p. 1037-1046.  
1498

1499 Veizer, J., Ala, D., Azmy, K., Bruckschen, P., Buhl, D., Bruhn, F., Carden, G.A.F., Diener, A., Ebner, S.,  
1500 Godderis, Y., Jasper, T., Korte, C., Pawellek, F., Podlaha, O.G., and Strauss, H., 1999,  $^{87}\text{Sr}/^{86}\text{Sr}$ ,  $\delta^{13}\text{C}$  and  
1501  $\delta^{18}\text{O}$  evolution of Phanerozoic seawater: *Chemical Geology*, v. 161, p. 59-88.  
1502

1503 Von Damm, K.L., 1990, Seafloor hydrothermal activity: black smoker chemistry and chimneys: *Annual*  
1504 *Reviews, Earth and Planetary Science*, v. 18, p. 173-204.  
1505

1506 Walshaw, R., Menuge, J., and Tyrrell, S., 2006, Metal sources of the Navan carbonate-hosted base  
1507 metal deposit, Ireland: Nd and Sr isotope evidence for deep hydrothermal convection: *Mineralium*  
1508 *Deposita*, v. 41, p. 803-819.  
1509

1510 Watson, J., 1978, The basement of the Caledonide orogen in Britain: *Canada Geological Survey Paper*  
1511 78-13, p. 75-77.  
1512

1513 Wilkinson, J.J., 2001, Fluid inclusions in hydrothermal ore deposits: *Lithos*, v. 55, p. 229-272.  
1514

1515 Wilkinson, J.J., 2003, On diagenesis, dolomitisation and mineralisation in the Irish Zn-Pb orefield:  
1516 *Mineralium Deposita*, v. 38, p. 968-983.

1517

1518 Wilkinson, J.J., and Earls, G., 2000, A high temperature hydrothermal origin for black dolomite matrix  
1519 breccias in the Irish Zn-Pb orefield: *Mineralogical Magazine*, v. 64, p. 1077-1096.

1520

1521 Wilkinson, J.J., Boyce, A.J., Everett, C.E., and Lee, M.J., 2003, Timing and depth of mineralization in  
1522 the Irish Zn-Pb orefield, in Kelly, J.G., Andrew, C.J., Ashton, J.H., Boland, M.B., Earls, G., Fusciardi, L.,  
1523 and Stanley, G., eds., *Europe's Major Base Metal Deposits: Dublin, Irish Association for Economic*  
1524 *Geology*, p. 483-497.

1525

1526 Wilkinson, J.J., Everett, C.E., Boyce, A.J., Gleeson, S.A., and Rye, D.M., 2005a, Intracratonic crustal  
1527 seawater circulation and the genesis of sub-seafloor Zn-Pb mineralization in the Irish orefield:  
1528 *Geology*, v. 33, p. 805-808.

1529

1530 Wilkinson, J.J., Eyre, S.L., and Boyce, A.J., 2005b, Ore-forming processes in Irish-type carbonate-  
1531 hosted Zn-Pb deposits: Evidence from mineralogy, chemistry and isotopic composition of sulfides at  
1532 the Lisheen Mine: *ECONOMIC GEOLOGY*, v. 100, p. 63-86.

1533

1534 Wilkinson J.J., Collins, S.J., and Jeffries, T., 2007, The composition of Irish-type Zn-Pb ore fluids, in  
1535 Andrew, C.J. et al., eds., *Digging Deeper, Proceedings of the 9<sup>th</sup> Biennial SGA Meeting: Dublin, Irish*  
1536 *Association for Economic Geology*, p. 279-282.

1537

1538 Wilkinson, J.J., Stoffell, B., Wilkinson, C.C., Jeffries, T.E., and Appold, M.S., 2009, Anomalously metal-  
1539 rich fluids form hydrothermal ore deposits: *Science*, v. 323, p. 764-767.

1540

1541 Wright, W.R., Johnson, A.W., Shelton, K.L., Somerville, I.D., Gregg, J.M., 2000, Fluid migration and  
1542 rock interactions during dolomitisation of the Dinantian Irish Midlands and Dublin Basin: *Journal of*  
1543 *Geochemical Exploration*, v. 69-70, p. 159-164.

1544

1545 Yardley, B.W.D., 2005, Metal concentrations in crustal fluids and their relationship to ore formation:  
1546 *Economic Geology*, v. 100, p. 613-632.

Table 1. Summary of microthermometric data from the Irish Orefield.

Location	Ref.	Minerals	n	Homogenization T (°C)			Salinity (wt% NaCl equivalent)			T <sub>m</sub> hyd	δ <sup>34</sup> S	Notes
				Mode(s)	Min	Max	Spread	Mode(s)	Min			
<b>DEPOSITS</b>												
Abbeytown	1	sp	3	100-110	105	123	18	10-11	10	11	1.0	-
	1	cc	18	130-140	88	180	92	12-13, 24-25	10	25	15.0	-
Navan	2	-	6	180-190	-	-	-	24	20	25	5.0	-
	3	dol, sp	40	130-140, 160-170	90	175	85	-	-	-	-	-
	4	sp	98	100-110, 140-150	75	176 <sup>†</sup>	101	5-6, 14-15, 24-25	5.4	26.2	20.8	-23.5
Tynagh	4	cc, dol, ba	85	120-130	73	171 <sup>‡</sup>	98	7-8, 20-21	5.6	25.2	19.6	-22.9
	5	-	303	150-160	90	230	200	8, 17	5	23	18.0	-
	6	sp	60	230-240	181	243	62	12-13	8.1	13.5	5.4	-
Galmoy	6	qz (a/g), ba	150	150-160	106	202 <sup>†</sup>	96	10-11, 16-17, 20-21	6.4	23.2	16.8	-
	4, 7	sp	78	160-170	129	179	50	11-12, 13-14	10.8	16.6	5.8	-22.4
	7	dol, cc	75	180-190	111	228	117	13-14	8.8 <sup>‡</sup>	20.9	12.1	-
Lisheen	8	sp	-	-	87	240	153	-	7	20	13.0	-
	8	dol	-	-	145	260	115	14-16	14	16	2.0	-
	4, 7	sp	282	170-180, 200-210	139 <sup>†</sup>	210 <sup>‡</sup>	71	4-5, 11-12, 13-14, 17-18	4.0	18.1	14.1	-22.6 <sup>††</sup>
Silvermines	7	cc, dol, qz	101	150-160, 200-210	123	277	154	12-13, 16-17	5.4	24.6 <sup>††</sup>	19.2	-22.7
	4	sp	52	180-190	148	208	60	12-13, 17-18	12.1	19.3 <sup>†</sup>	6.8	-23.1
	9, 10	sp	35	170-180, 190-200	155	194	39	14-15	9.6	16.6 <sup>‡</sup>	7.0	-
Prospect	11	qz, sp, ba	8	180-190	190	280	90	-	-	-	-	-
	9, 10	qz, cb, ba	331	170-180, 190-200	72 <sup>‡</sup>	248 <sup>†</sup>	176	15-16, 18-19	8.3 <sup>‡</sup>	27.5	19.2	-
<b>PROSPECTS</b>												
Tatestown	2	-	26	180-190	90	210	120	10-12	10	12	2	-
	2	-	48	140-150	130	180	50	11, 18	-	-	-	-
Keel	12	sp	11	180-190	176	185	9	11-12	9.2	11.7	2.5	-
	13	sp	-	110-120	117	123	6	-	17	22	5.0	-6.5
Keel fault, Garrycam	4	sp	47	120-130	192	85	14-15, 9-10	6.0	16.5 <sup>‡</sup>	10.5	-	-23.9
	14	qz	8	180-190	196	98	5-6	4.4	9.1	4.7	-	-
Garrycam	15	sp	25	~130	110	187	77	-	18.4	24.2	5.8	-
	15	dol	6	~140	136	159	23	-	-	-	-	-
Moyvoughly	15	dol, ba	-	-	146	286	140	-17	-	-	-	-
	2	-	229	190-200	120	240	120	9	-	-	-	-
Harberton Bridge	16	-	-	~100	-	-	-	-	-	-	-	-
	17	cc	29	60-70	48	70	22	15-16	9.8	20.1	10.3	-22.1, -34.7
Kinnitty	18	cc	36	50-60	44	76	32	20-21	8.7	22.5	13.8	-21.3
	19	sp	6	170-180	171	212	41	14-15	13.9	14.9	1.0	-
Coolleen	19	dol	39	180-190	129	225	96	13-14	10.8	17.6	6.8	-
	19	cc	34	150-160	95	177	82	11-12, 13-14	4.8	14.2	9.4	-
Rathdowney prospects	7	dol	67	180-190, 210-220, 250-260	155	267	112	11-12, 13-14	1.4	22.4	21.0	-22.7
	7	sp	23	170-180	158	184 <sup>††</sup>	28	10-11, 16-17	10.4	17.9	7.5	-22.7
Derrykearn	20	sp	-	-	228	43	228	13	18	5.0	-	-
	20	dol	-	-	157	169	32	-14	-	-	-	-
Courtbrown	21	cc	40	170-180	160	190 <sup>‡</sup>	30	-	-	-	-	-
	4	sp	3	-	141	172	31	16-17	13	16.1	3.1	-24.0
Pallas Green	22	cc	18	150-160, 130-140	94	181	87	10-12	-	-	-	-
												11.0(sp), 10.5(sp), 11.5(qn)
<b>REGIONAL CARBONATES</b>												
Newcastle West	23	qz	-	-	160	190	30	-	-	-	-	-
	23	dol	-	-	160	200	40	-	-24	-	-	-
Midlands	24	dol, cc	-	250-260	164	271	107	11-12, 16-17 <sup>†</sup>	1.4	18.9	17.5	-
	24	dol, cc	-	120-130, 140-150 <sup>‡</sup>	55	209	154	2-3 <sup>†</sup> , 8-9, 9-10 <sup>‡</sup>	0	16.2	16.2	-
Midlands	24	dol, cc	-	90-100, 140-150 <sup>‡</sup>	59	170 <sup>‡</sup>	111	25-26	17.9	35.9	18.0	-
	4	dol	46	140-150, 190-200	135	236	101	12-13	9.2	14.7	5.5	-
Midlands	4	dol	43	180-190, 220-230	175	257	82	12-13	10.5	14.2	3.7	-
	4	dol	90	130-140	81	159 <sup>‡</sup>	78	30-31 <sup>†</sup>	24.1 <sup>†</sup>	32.8 <sup>†</sup>	5.7	-1.7
Midlands	4	pink dol	49	90-100, 120-130	89	137 <sup>‡</sup>	48	23-25	23.0	28.7	8.7	-17.9
												Pink dolomite, drillhole samples 97-3476-01
<b>BASEMENT</b>												
SW Midlands area	4, 25	sp	71	150-160, 210-220	135 <sup>‡</sup>	224	89	11-12, 13-14, 16-17	11.2 <sup>‡</sup>	18.1	6.9	-23.2
	4, 25	qz, cc, dol, ba	585	170-180	101 <sup>††</sup>	238	137	10-11, 13-14, 17-18	8.4 <sup>††</sup>	20.6 <sup>††</sup>	12.2	-22.7

\*?Numbers of outliers unknown (incomplete bivariate plot)

n - Number of inclusions measured for Th; in most cases the number of salinity estimates will be less

† - Th values in euhedral ore-stage quartz at Tynagh extend up to 314°C with salinities of 7.0-24.8 wt%; high Th values in barite ignored

‡ - Modes unavailable; only ranges given

‡ - From sub-Waulsortian samples

‡ - From supra-Waulsortian samples

# - Salinities estimated from final ice melting temperatures using metastable extension of ice liquidus; these are underestimated by <8 % relative to NaCl-CaCl<sub>2</sub> modelling.

- not available

References: 1. Hitzman (1986); 2. Probert (1983); 3. Peace et al. (2003); 4. This study; 5. Unknown, erroneously referenced as Boast (1981) in Andrew (1993); 6. Banks and Russell (1992); 7. Eyre (1998); 8. Thompson et al. (1992); 9. Samson and Russell (1983); 10. Samson and Russell (1987); 11. Greig et al. (1971); 12. Roedder (1976); 13. Caulfield et al. (1986); 14. Collins (unpublished); 15. Thompson (1992) cited in Slowey et al. (1995); 16. Finlow-Bates, pers. comm. in Emo (1986); 17. Trude and Wilkinson (2001); 18. Strongman (unpublished); 19. Lee (2002); 20. Unknown, cited in Hitzman and Beaty (1996); 21. Reed and Wallace (2001); 22. Crowther and Wilkinson (unpublished); 23. Mulhall (2003); 24. Johnson et al. (2009); 25. Everett et al. (1999a).

## Figure Captions

Fig. 1. Simplified geological map of Ireland showing localities mentioned in the text (numbered). 1. Abbeytown; 2. Tatestown; 3. Navan; 4. Keel; 5. Garrycam; 6. Moyvoughly; 7. Ballinasloe; 8. Tynagh; 9. Newcastle West; 10. Harberton Bridge; 11. Stradbally; 12. Kinnitty; 13. Derrykearn; 14. Durrrow; 15. Ballyragget No. 1 borehole; 16. Rathdowney East; 17. Lisheen; 18. Galmoy; 19. Holycross; 20. Fantane; 21. Latteragh; 22. Silvermines; 23. Birdhill; 24. Ballycar; 25. Tobermalug; 26. Castlegarde; 27. Caherconlish South; 28. Srahane West; 29. Courtbrown; 30. Meelin No. 1 borehole; 31. Rocky Island. Modified after the Mineral Deposits of Ireland map (CSA Ltd and the Geological Survey of Ireland, 1994) and Everett et al. (2003).

Fig. 2. Summary of cementation and mineralization paragenesis in the Irish Midlands Basin. Modified from Wilkinson et al. (2003) and incorporating observations from Eyre (1998), Wilkinson and Earls (2000), Gregg et al. (2001), Reed and Wallace (2001), Lee and Wilkinson (2002) and Wilkinson et al. (2005b). The area filled with the breccia symbol indicates the range of paragenetic stages that are observed incorporated as clasts in synsedimentary breccias; the light grey field indicates the approximate timing of formation of undulose, subhorizontal solution seams (broadly synchronous with the onset of main hydrothermal activity); the hatched field indicates the main period of hydrothermal activity; and the dark grey field indicates the approximate timing of late, conventional stylolites (variable orientations).

Fig. 3. Plots of homogenization temperature as a function of maximum inclusion dimension for: (A) Lower Paleozoic-hosted feeder veins; (B) Regional Lower Carboniferous carbonate cements; (C) Mineral deposits. Data from Everett et al. (1999a) and Wilkinson (unpublished).

Fig. 4. Sketches of fluid inclusion assemblages from carbonate cements illustrating consistent microthermometric properties (homogenization temperatures and final ice melting temperatures), and systematic changes in relation to crystal growth zones. (A) Fine-grained replacement dolomite hosting LP<sub>1</sub> fluids displaying decreasing salinity and increasing T<sub>h</sub> during growth. (B) Medium- to coarse-grained dolomite with core hosting B<sub>3</sub> brines and overgrowth hosting B<sub>2</sub> brines. Arrows indicate growth direction; dashed lines depict growth zones. Brackets indicate anomalous T<sub>h</sub>, possibly due to leakage.

Fig. 5. Plot of Na# ( $\text{NaCl}/[\text{NaCl}+\text{CaCl}_2]$ ) versus total salinity (wt% NaCl+CaCl<sub>2</sub> equivalent) based on ice and hydrate melting temperatures in fluid inclusions. Fields for Lower Paleozoic vein-hosted fluids (LP<sub>1</sub>), deposit sphalerite-hosted ore fluids (LP<sub>2</sub>) and inferred brine compositions are shown. Possible processes controlling variations in composition are indicated (see text for details). Data from one Silvermines sphalerite sample (BH K22/188') containing brine inclusions (Samson and Russell, 1987) and average data for barite and

Group 2 and 3 inclusions from Tynagh (Banks and Russell, 1992) are also shown. Comparative Southwest England brine data are from Stoffell et al. (2004) and Dead Sea brines from Klein-BenDavid et al. (2004).

Fig. 6. Halogen systematics of Irish fluids. (A) log Br versus log Cl plot; (B) Cl/Br versus Na/Br; (C) Cl/Br versus Ca/Br. Possible mixing and exchange trajectories are shown. Dashed lines in (B) represent 25 and 50% Na loss from evaporated seawater precursors. Seawater evaporation trajectory from McCaffrey et al. (1987). Compositions of modern seawater and seawater-derived brine with an evaporation ratio of 25x are shown for reference (stars).

Fig. 7. Range of major, minor and trace element compositions of LP<sub>1</sub> fluids (mean values from Fantane, Latteragh, Birdhill and Ballycar; Wilkinson et al., 2005a and unpublished) normalized to an evaporated seawater precursor (prior to gypsum precipitation). This illustrates the element gains/losses undergone by partially evaporated seawater during basement circulation. A range of ocean ridge vent fluid compositions are shown for comparison, normalized to a normal seawater precursor (data from TAG, MARK-1, MARK-2 and 21°N OBS; Von Damm, 1990).

Fig. 8. Calculated  $\delta^{18}\text{O}$  and measured  $\delta\text{D}$  compositions of water trapped in quartz-hosted fluid inclusions from Lower Paleozoic-hosted veins compared with results from Silvermines (Samson and Russell, 1987). Possible Lower Carboniferous seawater composition derived from data in Veizer et al. (1999) and assuming consistent relationship between seawater oxygen and hydrogen isotope compositions and a constant global meteoric water line. Seawater evaporation trajectory from Knauth and Beeunas (1985) and shown for both modern seawater (green) and possible Lower Carboniferous seawater (blue) starting points. Solid sausage-shaped fields indicate compositions for seawater partially evaporated to the degree inferred for the LP<sub>1</sub> fluids. Dashed curves illustrate modeled exchange trajectories for the extremes of the two fields, calculated at 200 and 300 °C. Range and mean Lower Paleozoic wholerock compositions from Thomas et al. (1985). Rock-fluid fractionation factors ( $\Delta_{r-w}^{\text{O}} = 7.0, 3.4$  at 200 and 300 °C respectively;  $\Delta_{r-w}^{\text{H}} = -32.6, -33.2$  at 200 and 300 °C respectively) estimated using the approach outlined in Samson and Russell (1987). Most of the LP<sub>1</sub> fluid compositions can be explained by small degrees of mixing between fully basement-equilibrated fluids with low  $\delta\text{D}$  brines, possibly produced by strong evaporation (25x evaporation ratio) of  $^{18}\text{O}$ - and D-depleted Lower Carboniferous seawater. The higher temperature Silvermines orefluids (LP<sub>2</sub>) do not fit the modeling implying use of inappropriate fractionation factors or, potentially, exchange with unusually low  $\delta\text{D}$  basement rocks.

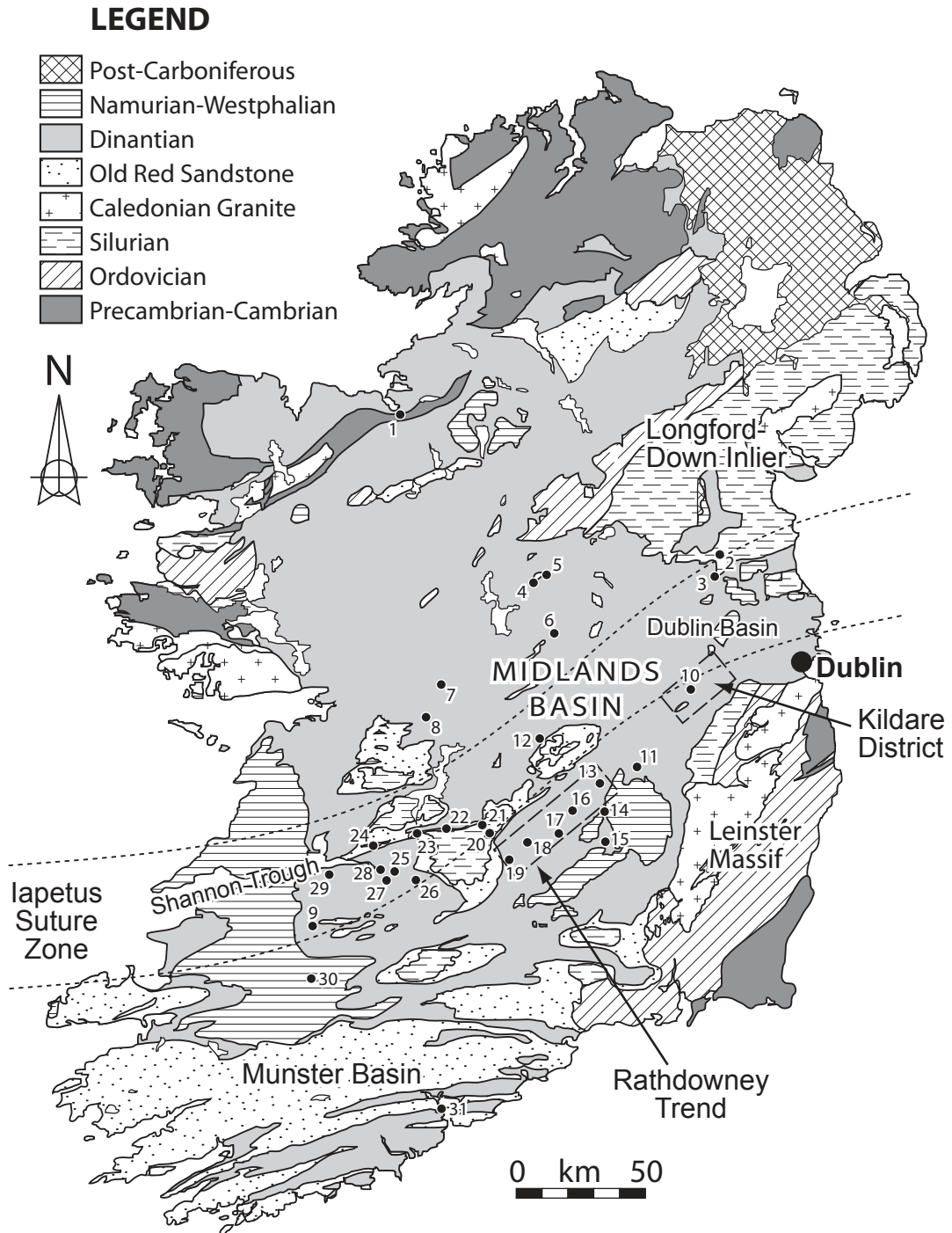
Fig. 9. Modal homogenization temperature-salinity plot for all localities in the Irish Midlands based on the data compiled in Table 1. With a few exceptions, localities north and west of the Iapetus Suture plot in the lower left of the diagram and those from the south and east plot in the upper right suggesting a broad



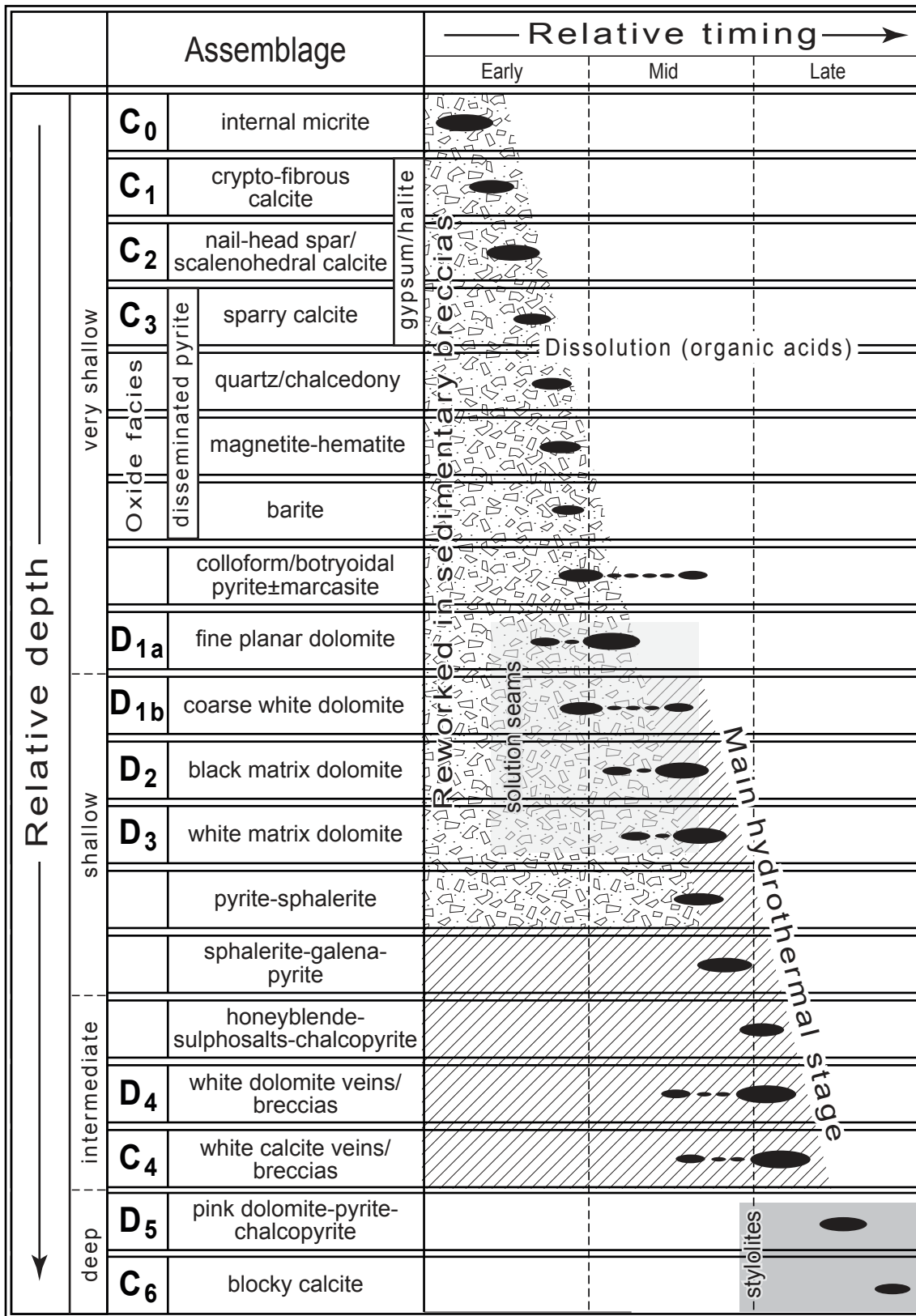
division into two main flow compartments. Exceptions are: low temperature brines at Navan that are at least partly post-ore because they occur in late stage vug-filling cements and in veins that extend far into the hanging wall stratigraphy; and high temperature, sphalerite-hosted inclusions at Tynagh (Banks and Russell, 1992).

Fig. 10. Diagrams illustrating fluid processes and controls on mineralization. A. Schematic cross-section illustrating processes responsible for generation of fluid types and chemical exchange during crustal circulation. Note approximate 2x vertical exaggeration; B. Three-dimensional cartoon representation of fault arrays, seafloor topography and mixing processes operating in the ore-forming environment. White arrows indicate possible brine migration pathways from uplifted footwall into hanging wall depressions via relay ramps; C. Representation of paleogeography in the Irish Midlands showing localization of deposits (red areas represent projection of massive sulfide lenses to the paleoseafloor) on the basinward side of fault-controlled shelves/islands where strongly evaporated bittern brines were generated.

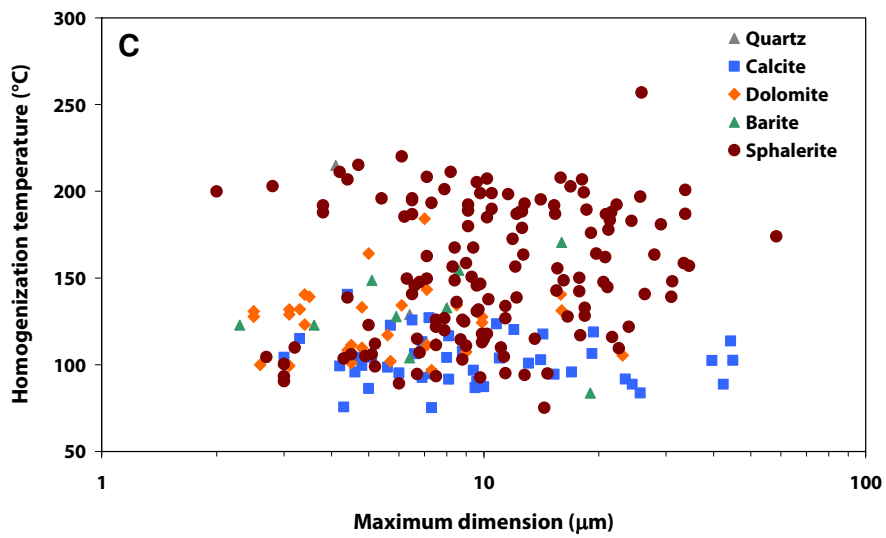
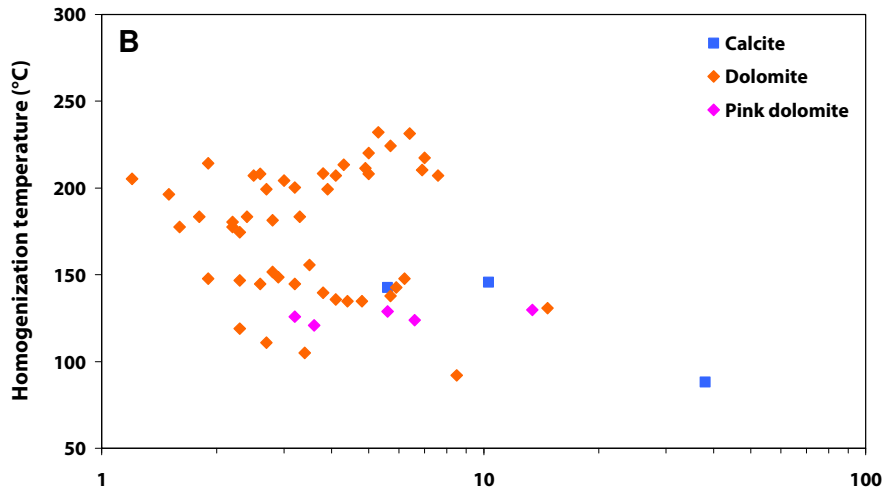
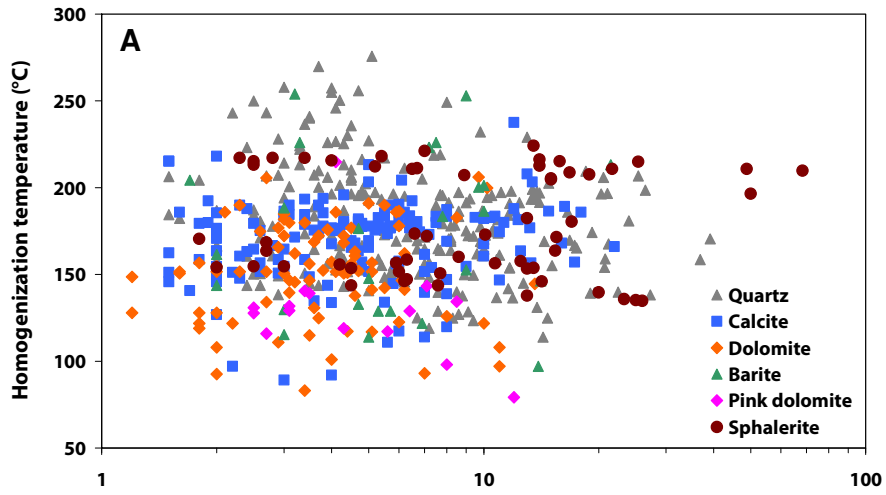
Wilkinson\_Fig. 1

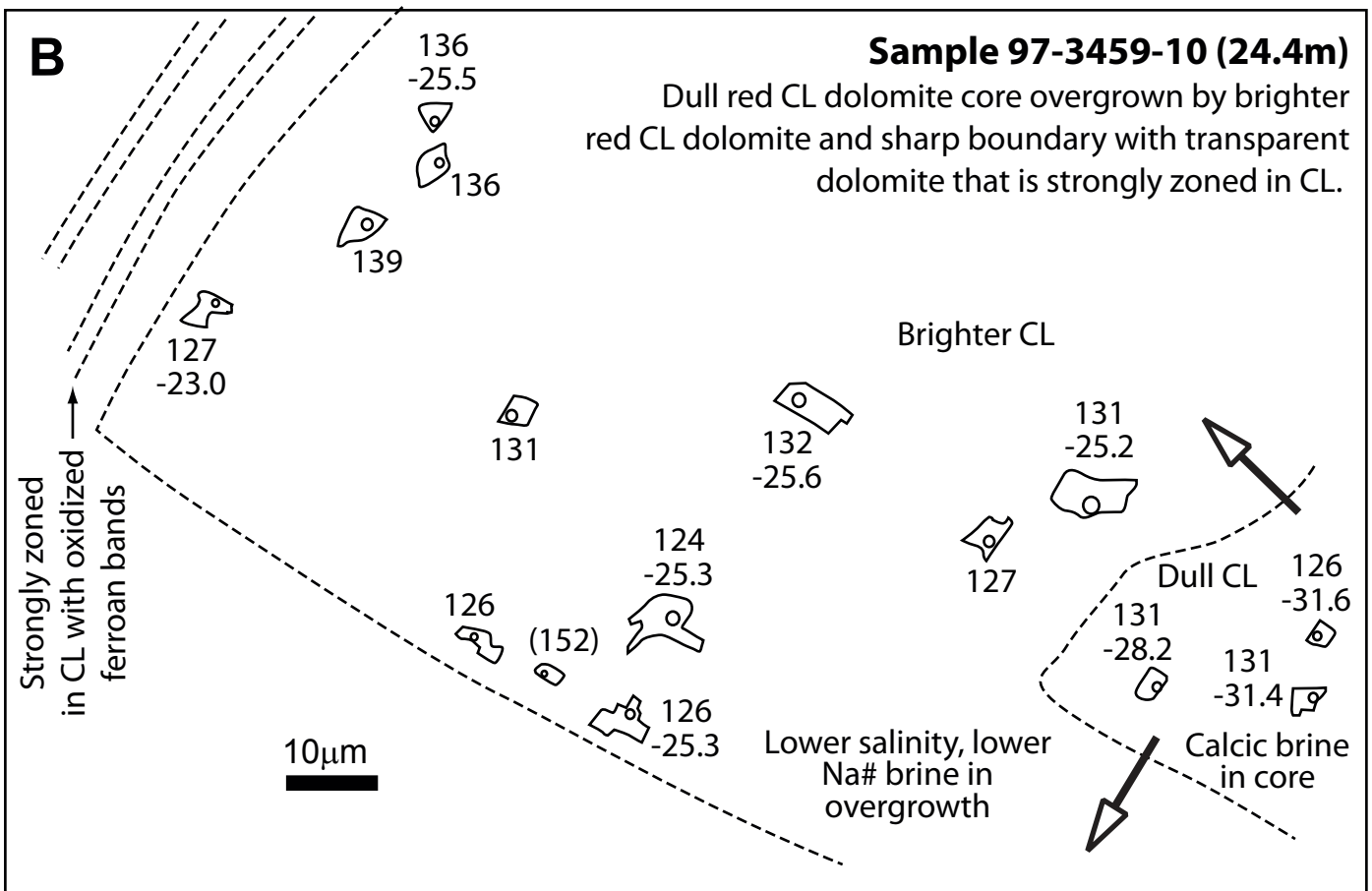
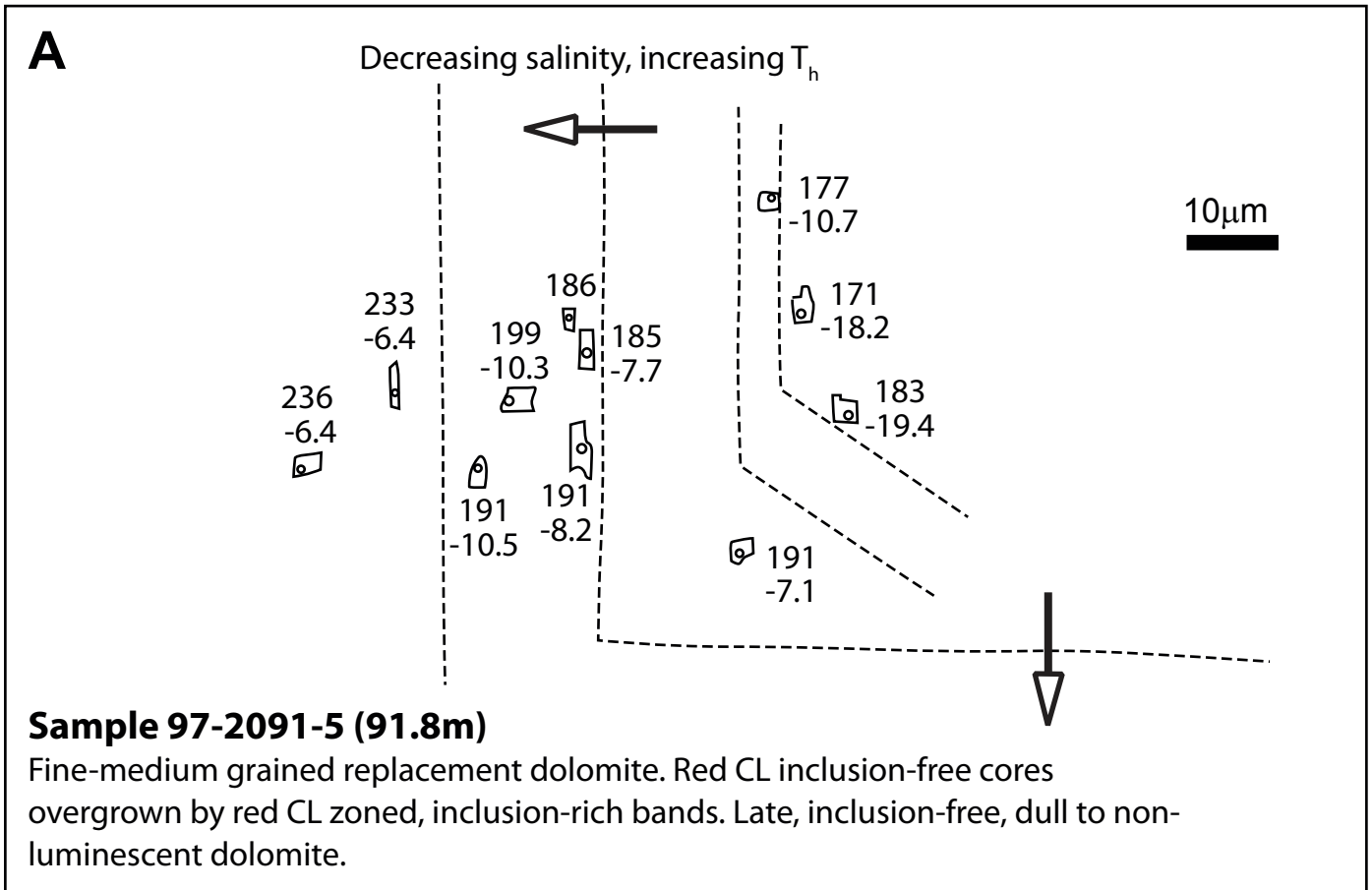


Wilkinson\_Fig. 2

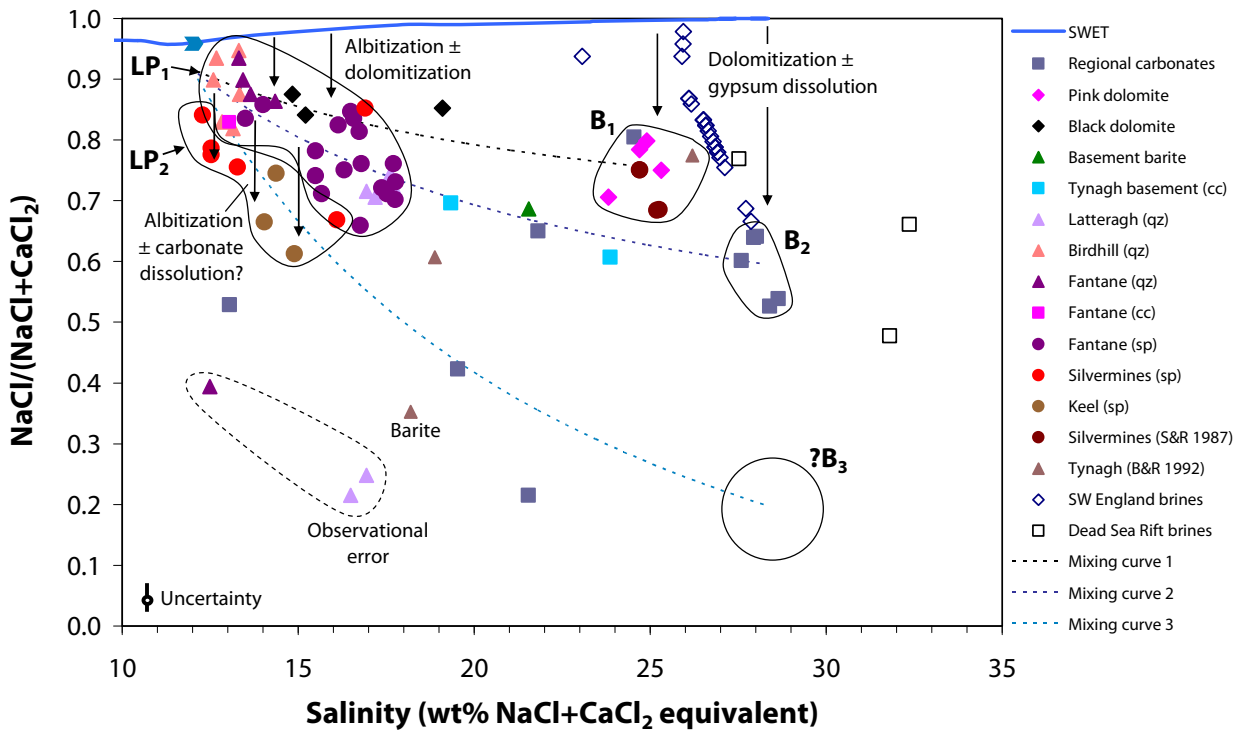


Wilkinson\_Fig.3

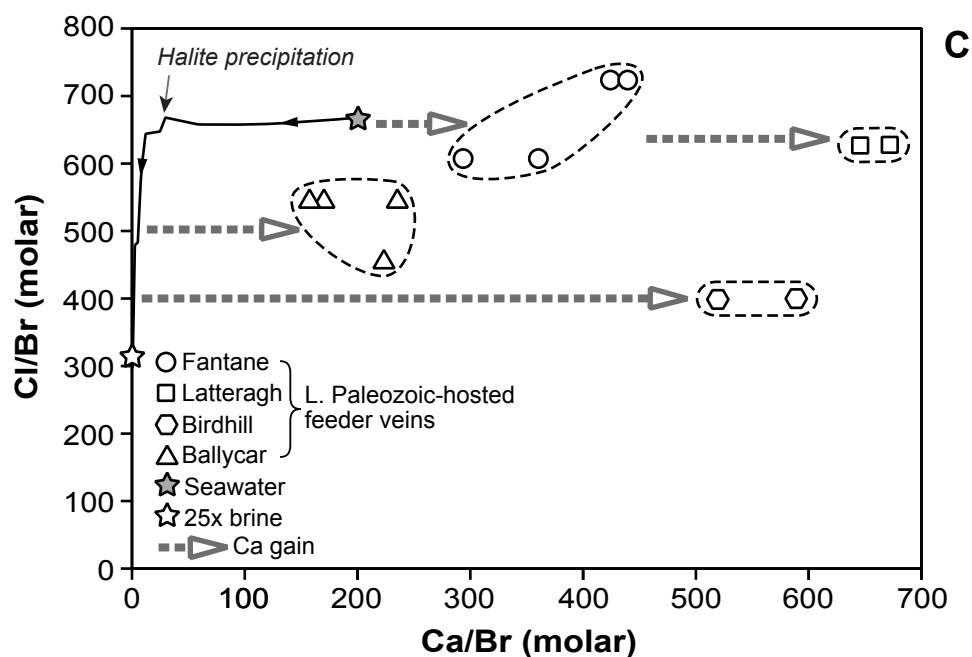
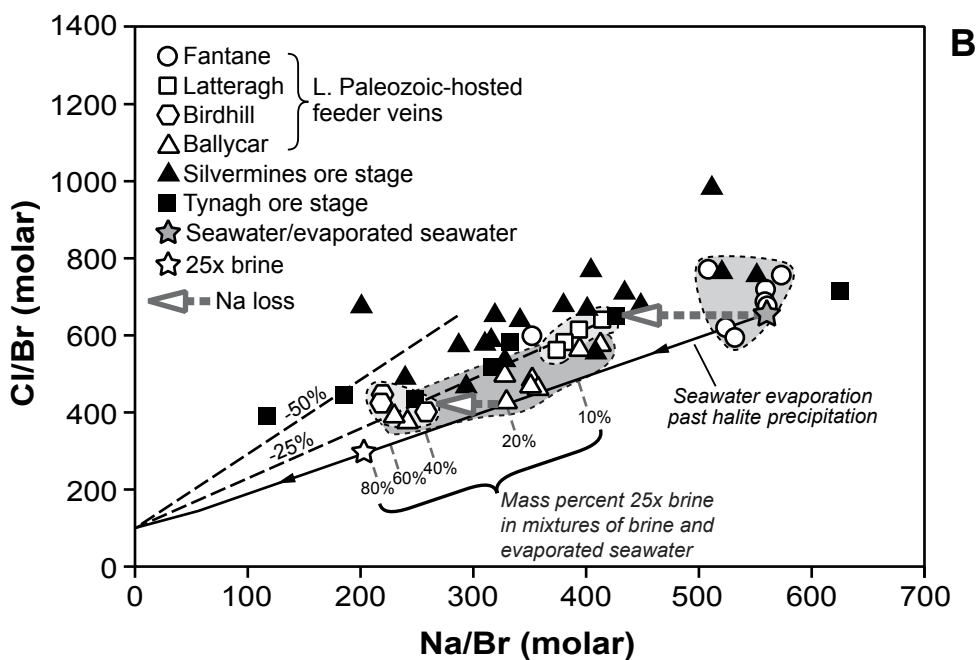
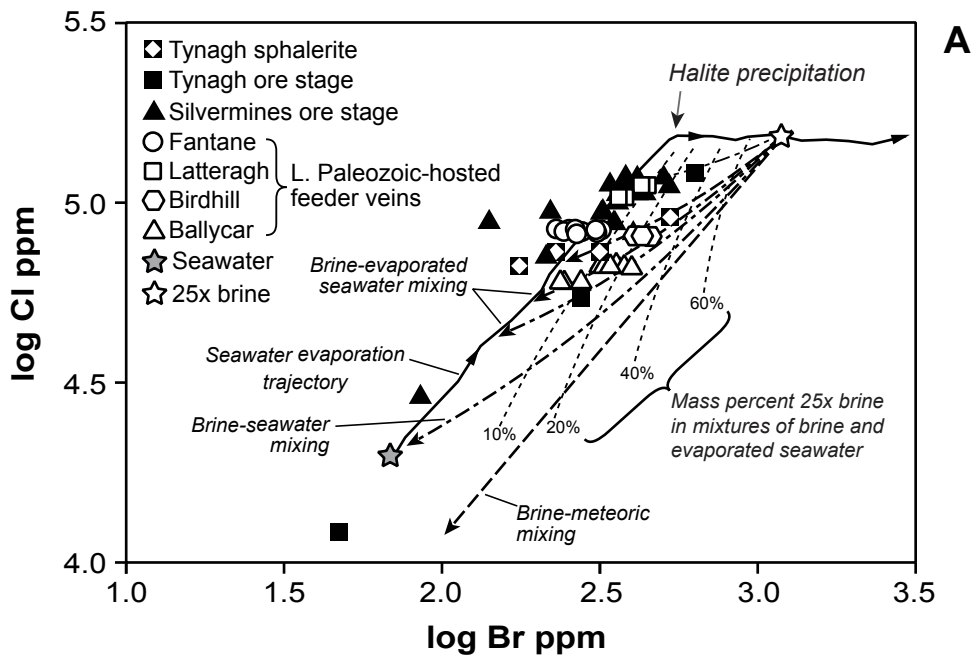




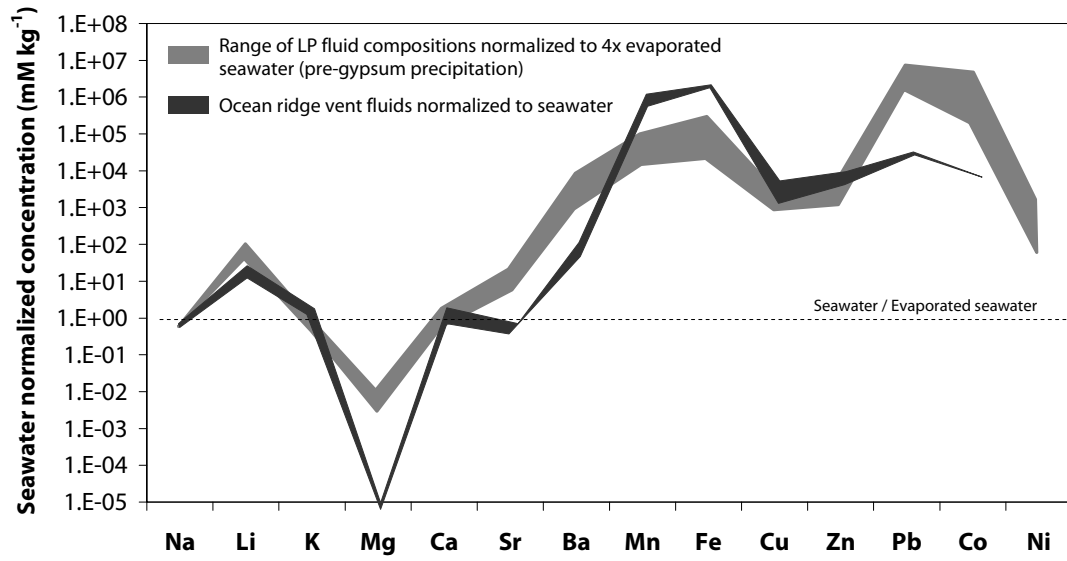
Wilkinson\_Fig.5



Wilkinson\_Fig. 6

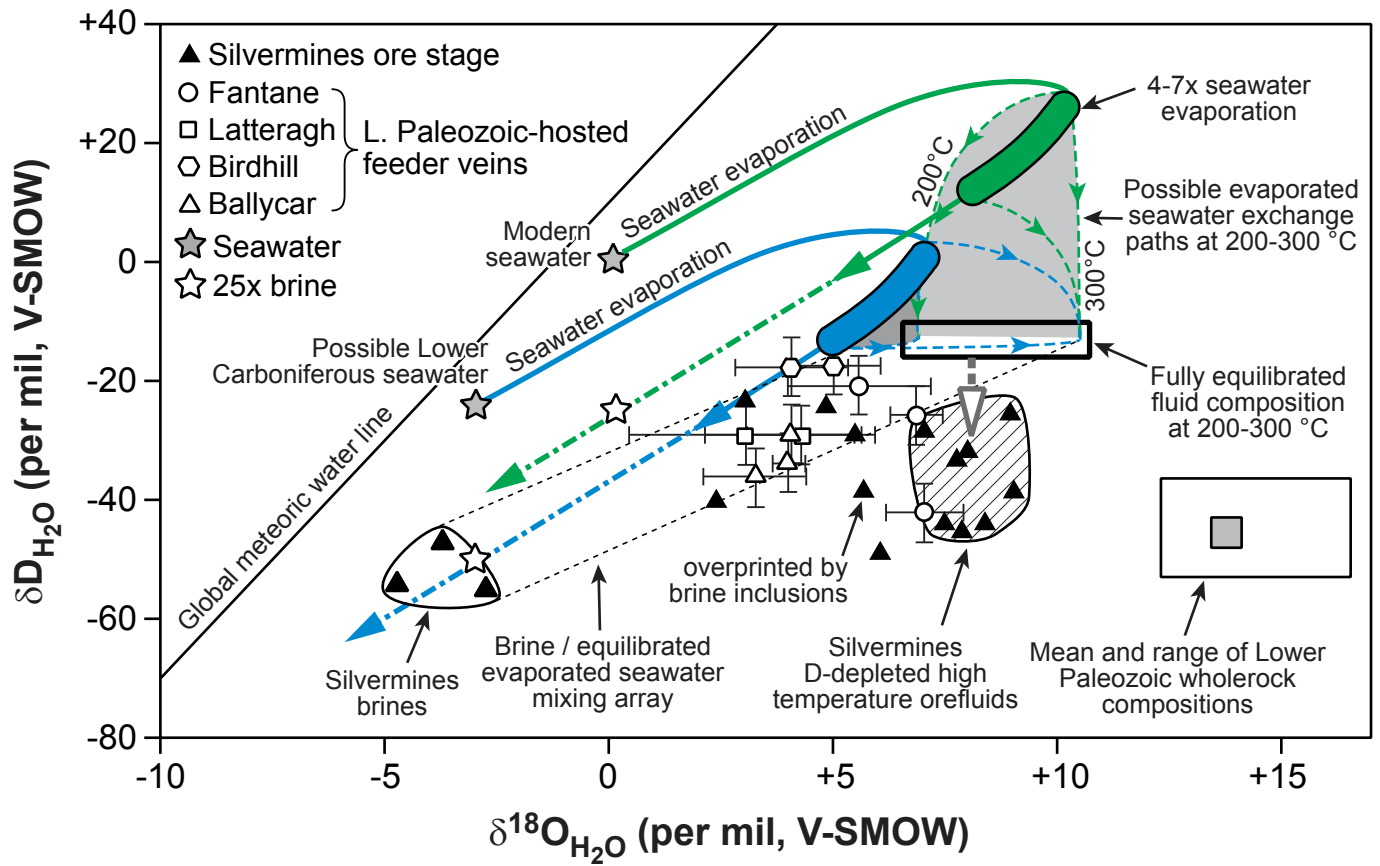


Wilkinson\_Fig. 7





Wilkinson\_Fig.8



Wilkinson\_Fig.9

